DSPACE

https://dspace.org/

Taxonomic and taphonomic interpretations of newly excavated in situ GD 2 faunal remains at Gondolin

Engelbrecht, Micke; Val, Aurore; Kibii, Job M.; Steininger, Christine

2024-01
The Evolutionary Studies Institute
https://hdl.handle.net/10539/37327

Downloaded from a DSpace repository. https://dspace.org/

Taxonomic and taphonomic interpretations of newly excavated *in situ* GD 2 faunal remains at Gondolin

Micke Engelbrecht[1] §, Aurore Val[1,2*], Job M. Kibii[1,3] & Christine Steininger[1]

[1]*Evolutionary Studies Institute, School of Geosciences, University of the Witwatersrand, Private Bag 3, WITS, Johannesburg, 2050 South Africa*
[2]*Department of Early Prehistory and Quaternary Ecology, University of Tübingen, Schloss Hohentübingen, 72070, Tübingen, Germany*
[3]*Earth Sciences Department, National Museums of Kenya, P.O. 4065-001000, Nairobi, Kenya*

Received November 2019. Accepted 1 May 2023

Gondolin is one of the fossil-bearing karstic localities in the Cradle of Humankind, South Africa. Periodic excavations of calcified and decalcified sediments at several loci (GD 1, GD 2 and GD A) over the last few decades have yielded a sizeable sample of Plio-Pleistocene fauna, including two hominin teeth from *ex situ* deposits. In 2015, renewed excavations were conducted at the GD 2 locality, which consists of decalcified *in situ* deposits, in order to shed more light on the site's complex formation processes as well as to try finding new hominin material from a stratigraphically secured context. While these excavations did not yield any hominin material, abundant macrovertebrate remains were recovered. This paper presents the taxonomic composition and taphonomic characteristics of this new faunal assemblage. The occurrence of *Equus* sp. as well as the extinct species *Metridiochoerus andrewsi* and *Hystrix makapanensis* places the assemblage in a depositional age bracket of 2.33–1.78 Ma, which is consistent with ages already proposed for GD 2. No primate material was recovered. The assemblage displays a taxonomic and bodyweight bias towards small-bodied (size classes I and II) bovids. The taphonomic characteristics of the bovid remains suggest the selective action of a leopard-like carnivore and while there is no direct evidence that the locality was used as a hyaena den, secondary scavenging by hyaenids cannot be excluded. Porcupines played an ancillary role in the bone accumulation. We performed intra- and inter-site taxonomic and taphonomic comparisons between this faunal sample and fossil assemblages from previously excavated localities at Gondolin (GD 1, GD 2 and GD A), as well as from other *Paranthropus robustus*-bearing sites in the Cradle of Humankind. These comparisons indicate that this new sample closely resembles the faunal assemblage previously collected from *in situ* calcified sediments at the GD 2 locality, in terms of species composition, bovid size class distribution, carnivore to ungulate ratio, and general taphonomic characterization.

Keywords: Plio-Pleistocene, South Africa, Cradle of Humankind, *Hystrix makapanensis*, *Metriodiochoerus andrewsi*, *Paranthropus robustus*.

Palaeontologia africana 2023. ©2023 Micke Engelbrecht, Aurore Val, Job M. Kibii & Christine Steininger. This is an open-access article published under the Creative Commons Attribution 4.0 Unported License (CC BY4.0). To view a copy of the license, please visit http://creativecommons.org/licenses/by/4.0/. This license permits unrestricted use, distribution, and reproduction in any medium, provided the original author and source are credited.
The article is permanently archived at: https://hdl/handle.net/10539/37327

INTRODUCTION

Brief presentation of the site and history of past excavations

Gondolin palaeocave is located on the edge of the Cradle of Humankind, 4 km southwest of the town of Broederstroom and 20 km northwest of the Sterkfontein Caves (Fig. 1A). Gondolin contains one of the largest karstic-derived Plio-Pleistocene faunal assemblages in South Africa (Adams 2010). Besides Gladysvale (Berger *et al*. 1993), it is the only other site formed in the Eccles Formation to have yielded early hominin fossils. Gondolin is also the only site in southern Africa to contain *Paranthropus* remains comparable in size to *Paranthropus boisei* from East Africa (Menter *et al*. 1999).

The first phase of excavations, conducted by Vrba in 1979, resulted in the removal of approximately 2 m^3 of highly fossiliferous *in situ* calcified siltstone breccia from a hanging remnant in the northeastern cave wall (Vrba 1982; Fig. 1B). This area is referred to as GD 2 (Adams 2006) given the deposit's proximity to the GD 2 datum point. It has yielded abundant fauna, initially described by Watson (1993a) and analysed in detail more recently (Adams 2006, 2010, 2012a,b; Adams & Conroy 2005). While large (95 549 specimens) and taxonomically diverse (27 taxa) (Adams 2006, 2010), the GD 2 assemblage does not contain hominin or non-hominin primate remains. In 1997, a second phase of excavations in large *ex situ* breccia dumps designated Gondolin Dump A or GD A (Fig. 1B; Menter *et al*. 1999) yielded a variety of fauna including mostly ungulates and, to a much lesser degree, carnivores, porcupines, and non-hominin primates (Adams 2006, 2018). These excavations identified the first and only two hominin remains from Gondolin, including the largest *Paranthropus robustus* lower second molar (GDA-2) documented in South Africa to date (Menter *et al*. 1999; Adams 2018). The third phase of excavations in 2003 focused on *in situ* decalcified deposits on the northern wall, designated GD 1 (Menter *et al*. 1999). The GD 1 faunal assemblage consists of isolated ungulate teeth and fragmentary diaphyseal fragments and does not contain any hominin or non-hominin primates (Adams 2006; Adams *et al*. 2007).

*Author for correspondence. E-mail: aurore_val@yahoo.com

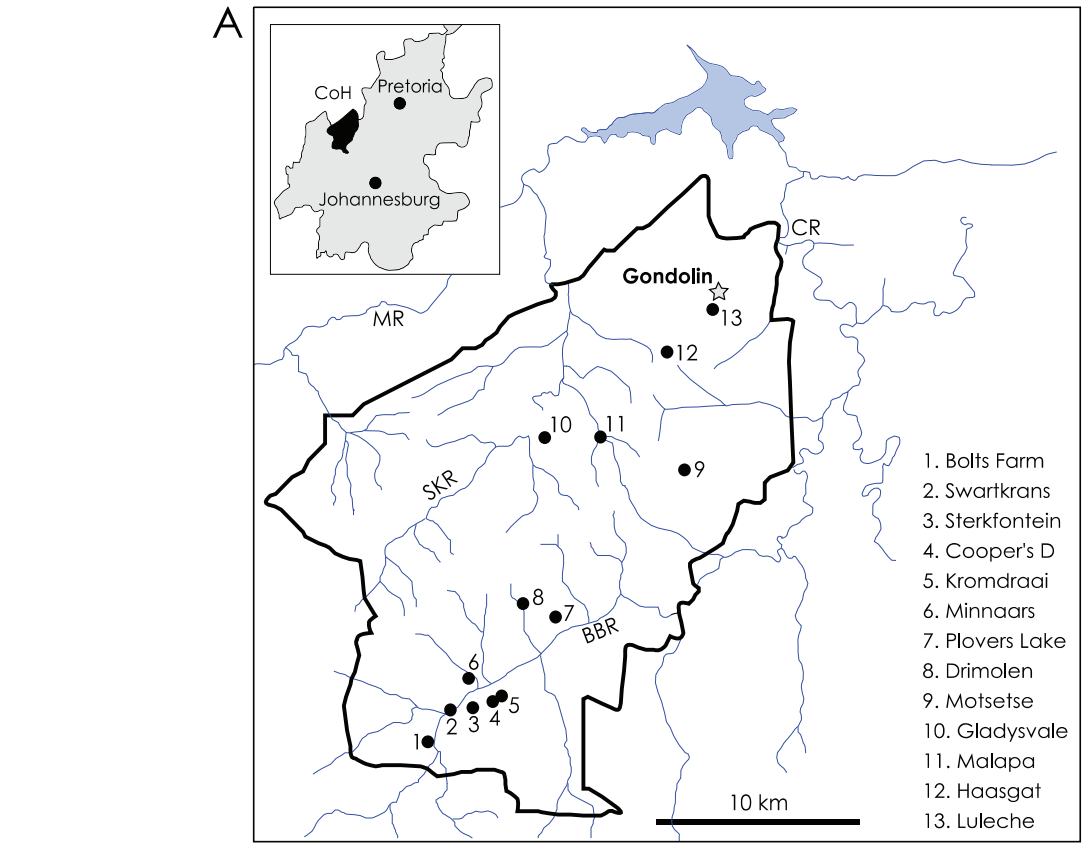

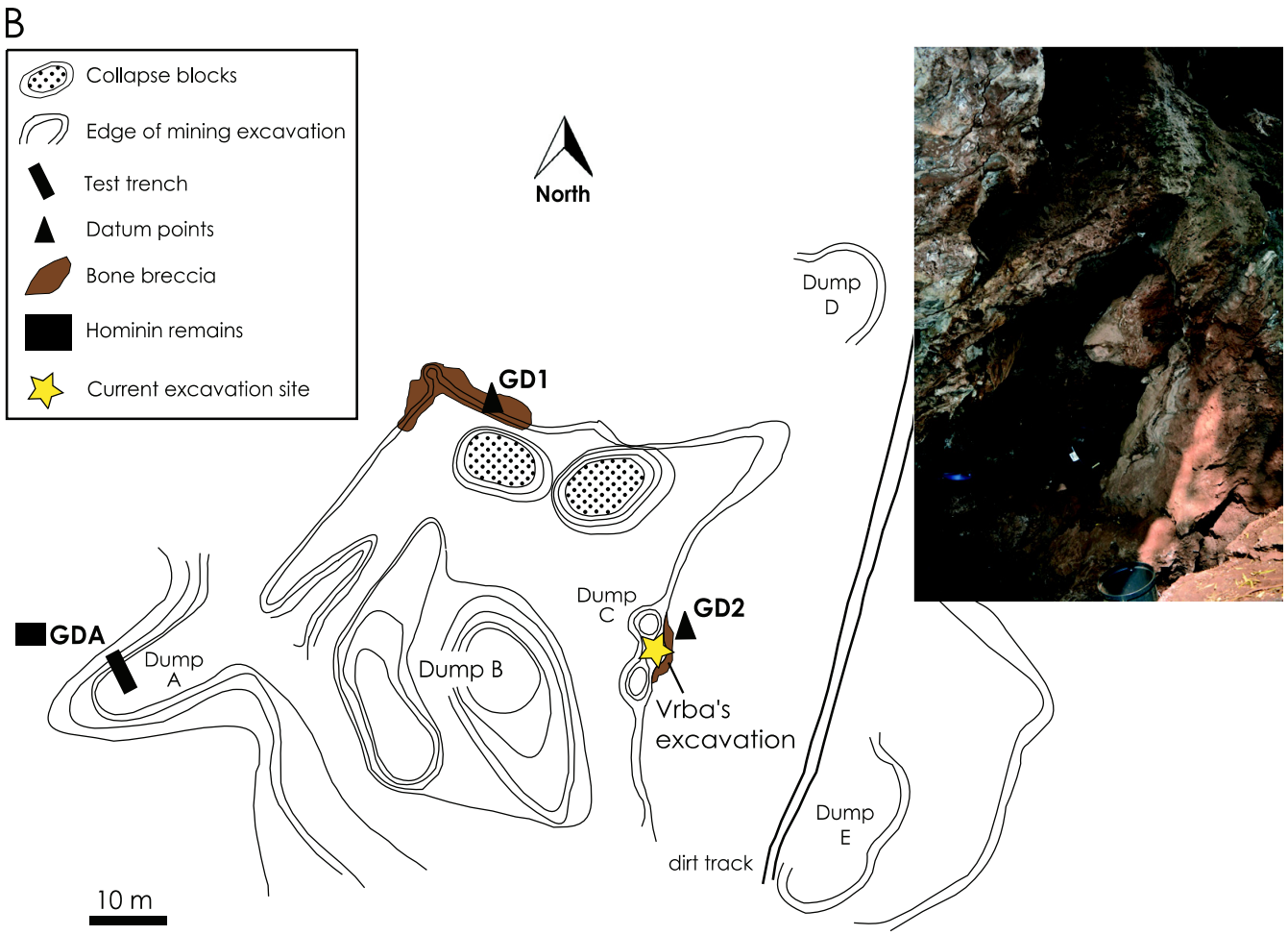

Figure 1. **A**, Geographic location of Gondolin in relationship to other Plio-Pleistocene fossil locations in the Cradle of Humankind, South Africa. **B**, Aerial site map of Gondolin and northwestern view of the new excavation area (after Menter *et al*. 1999, modified).

Existing ages for the fossil-bearing Gondolin deposits

Palaeomagnetism and biochronology have been applied to date the *in situ* fossiliferous deposits from Gondolin, i.e. GD 1 and GD 2. The presence of *Equus* suggests an age not greater than 2.36 Ma for GD1 (Bernor *et al*. 2010), a deposit that overlays a flowstone dated to the Olduvai normal polarity period at 1.95–1.78 Ma (Adams *et al*. 2007). GD 2 consists of two flowstones encasing a calcified clastic deposit. Correlation between the geomagnetic polarity time scale and the occurrence of *Metridiochoerus andrewsi* places the accumulation of the GD 2 faunal assemblage slightly before 1.78 Ma (Herries *et al*. 2006).

New excavations at the site and associated faunal assemblage

In an attempt to extend the sample of hominin remains from *in situ* deposits, as well as to further clarify site formation processes at Gondolin, two of us (J.M.K. and C.M.S.) initiated new excavations in 2015 at GD 2 under the auspices of Evolutionary Studies Institute (ESI), University of the Witwatersrand. Nineteen new, *in situ*, decalcified fossil deposits were identified and named according to their position (e.g. Upper East Wall, East Pit, etc.). This paper describes the taxonomic composition and presents the results of the taphonomic analysis of the macrofaunal assemblage recovered from these newly excavated GD 2 deposits. We also propose an age estimate for the deposit, based on faunal correlations. We refer to the newly excavated deposits and associated faunal assemblage as 'GD 2*' to avoid confusion with already published data on GD 2. The results are compared to those of the GD 1, GD 2 and GD A assemblages, as well as to other *Paranthropus*-bearing Plio-Pleistocene assemblages within the Cradle of Humankind, namely Kromdraai B/Member 2, Swartkrans Members 1 to 3, Coopers' D, Drimolen Main Quarry and Sterkfontein Member 5 East Infill.

MATERIALS AND METHODS

Excavation procedures

Excavations focused on *in situ* decalcified breccia deposits near the GD 2 datum point (Fig. 1B). The coordinates of all the anatomically identifiable, *in situ* macrofaunal specimens were recorded using a Total Station. Dry sieving of excavated sediment was done using 2 mm and 4 mm sieves. With the exception of the microfaunal remains, we incorporated the faunal material retrieved from the sieves alongside the plotted material for analysis. The specimens are curated at the ESI, University of the Witwatersrand. Accession numbers follow Zipfel & Berger (2009), with UW87- as the site number for Gondolin.

Taxonomic methods

We identified the specimens taxonomically and anatomically using comparative extant and extinct faunal collections of South African mammals, reptiles and birds housed at the ESI and the Ditsong National Museum of Natural History in Pretoria. Given the high degree of fragmentation of the postcranial material, taxonomic identification of bovid remains was based primarily on dental material. Most of the postcranial bovid material could not be identified to family or species level and was instead assigned to a size class following Brain (1974). When possible, we categorized the non-identifiable mammalian remains into three mammal size classes following Reynard *et al*. (2016). We recorded the element, skeletal portion, and side for the identifiable remains. We separated between juvenile and adult bone remains using epiphyseal fusion degree, and we considered dental eruption/wear to attribute the teeth to juvenile, adult or old adult individuals.

Taphonomic methods

We recorded abiotic and biotic modifications for the identified material, as well as for all unidentifiable elements ≥3 cm (n = 390). We firstly inspected bone surface modifications with the naked eye, which was followed by microscope analysis using an Olympus SZX16 at magnifications between ×0.67 and ×1.6. We inspected bone surfaces for damage related to the action of small to large avian and mammalian carnivores including hominins, rodent gnawing, invertebrates, root and rootlet acid etching, and water transport, using the available taphonomic literature (e.g. Maguire *et al*. 1980; Brain 1981; Shipman & Rose 1983a,b; Berger & Clarke 1995; Fisher 1995; Fernández-Jalvo & Andrews 2003; Domínguez-Solera & Domínguez-Rodrigo 2009; Backwell *et al*. 2012; Armstrong & Avery 2014; Cohen & Kibii 2015; Lloveras *et al*. 2008, 2012; Fernández-Jalvo & Andrews 2016). Each specimen was attributed a weathering stage, following Behrensmeyer (1978), as well as an estimate of manganese dioxide coating (i.e. 0%, <10%, 10–50% 50–90% and >90% of the bone surface covered). We used the methods developed by Villa & Mahieu (1991) to distinguish whether identifiable long bones and non-identifiable long bones ≥3 cm (n = 197) were fractured while green or dry. To estimate taxonomic composition of the assemblage as well as skeletal part representation, we calculated the Minimum Number of Elements (MNE), Minimum Number of Individuals (MNI), Minimum Animal Unit (MAU) and %MAU after Lyman (1994a). We sorted bone fragments into length categories (0.5–0.9 cm, 1.0–1.9 cm; 2.0–2.9 cm; ≥3 cm; ≥5 cm). We estimated the degree of fragmentation using the ratio of complete to fragmentary bones and the NISP/MNE ratio (Richardson 1980; Klein & Cruz-Uribe 1984). Bovid size classes I, II and III remains were divided into the five Voorhies groups as per their hydrological transport potential to test the possibility that the assemblage was hydrologically transported into the cave (Voorhies 1969). In order to investigate whether density-mediated attrition played a role in the skeletal part representation pattern, the %MAU values from the GD 2* bovid assemblage were plotted against the CT-derived bone mineral density (BMD) values of *Connochaetes taurinus* (blue wildebeest) provided in Lam *et al*. (1999). The shape-adjusted (BMD_2) values were used for the material, but the BMD_1 (not shape adjusted)

was used secondarily when the BMD_2 value was not available (Lam *et al*. 1999). Percentage MAU values were $\log_{10}$ transformed and a regression of %MAU on BMD was performed using a least-squares criterion. We acknowledge the limitations imposed by the use of blue wildebeest BMD values to a sample composed mostly of smaller bovids. These BMD values, however, are the only ones currently available to us and are used as a guideline. A similar procedure was adopted for *Hystrix makapanensis*, using BMD values of marmots (*Marmota monax* and *M. flaviventris*) from Lyman *et al*. (1992).

We considered several proxies to establish whether the GD 2* assemblage was accumulated by leopards and/or hyaenas, as proposed by Brain (1981), de Ruiter & Berger (2000), Pickering (2002) and Kuhn *et al*. (2010). Specifically, we considered the taxonomic composition and evenness of the faunal assemblage, the distribution of bovid material across size classes, the carnivore/ungulate ratio ([MNI (Carnivores) /MNI (Ungulates + Carnivores) × 100]), the mortality profiles and skeletal part representation for the bovid assemblage, as well as the nature and intensity of carnivore damage. We also considered the presence/absence of juvenile carnivore remains, presence/absence of bone cylinders, and presence/absence of coprolites.

We conducted an intra-site comparison of the GD 2* material with existing data on the GD 2, GD A and GD 1 assemblages (Adams 2006, 2010, 2018; Adams *et al*. 2007) by comparing taxonomic composition, carnivore to ungulate ratio, distribution of bovids across size classes and general taphonomic features between the different loci. We selected South African Plio-Pleistocene *Paranthropus robustus*-bearing sites for inter-site taxonomic and taphonomic comparisons using the same proxies. These sites include Sterkfontein Member 5 East Infill, Kromdraai B and Member 2, Swartkrans Member 1 (Hanging Remnant), Member 2, and Member 3, Cooper's D and Drimolen Main Quarry. We applied the McIntosh evenness index to evaluate the distribution of taxa within assemblages (McIntosh 1967). We used McIntosh values and carnivore to ungulate ratios as published in and/or calculated from Watson (1993b), Pickering (1999), de Ruiter (2003), de Ruiter *et al*. (2009), Adams (2010, 2018), Adams *et al*. (2016), and Fourvel *et al*. (2018).

RESULTS

Assemblage composition

The excavations yielded 11 542 fossil macrofauna specimens, of which 869 (7.5%) elements were identifiable below family level. A small percentage of material (3.3%) was classified as indeterminate mammal and artiodactyl remains. The remaining (89.2%) specimens consist of taxonomically unidentifiable animal bone and teeth fragments (n = 10 289). Table 1 presents the taxonomic composition of the GD 2* faunal assemblage. Nine mammalian families and a minimum of 16 taxa were identified. Besides, a few remains were attributed to reptilian and avian species, namely a testudine and the barn owl *Tyto alba*. Bovidae is the most common (45.2% of the NISP) and diverse family in the assemblage, with six tribes representing eight genera. It is also the family with the highest MNE (686) and MNI (23), ranging from mostly small to medium-bodied size bovids (classes I and II) to a single individual of a size class IV bovid. *Hystrix makapanensis* and *Hystrix africaeaustralis* have the second highest NISP (97) and MNE recorded (65). Other ungulates include two distinct equid taxa and suidae, represented by the extinct warthog *Metridiochoerus andrewsi*. Carnivore remains, attributed to a large hyaenid and a medium canid, are scarce in the assemblage, which results in a low carnivore to ungulate ratio of 7.4%. No primate material was recovered.

Systematic palaeontology

ORDER CARNIVORA Bowdich, 1821
Family HYAENIDAE Gray, 1821

Hyaenidae gen. et sp. indet.

Referred specimens: partial premolar crown (UW87-692; Fig. 2A).

Description: distal accessory cusp of a right fourth premolar of a hyaenid.

Family CANIDAE Fisher de Waldheim, 1817

Canidae gen. et sp. indet.

Referred specimens: thoracic vertebra (UW87-1871; Fig. 2B); right astragalus (UW87-1684; Fig. 2C).

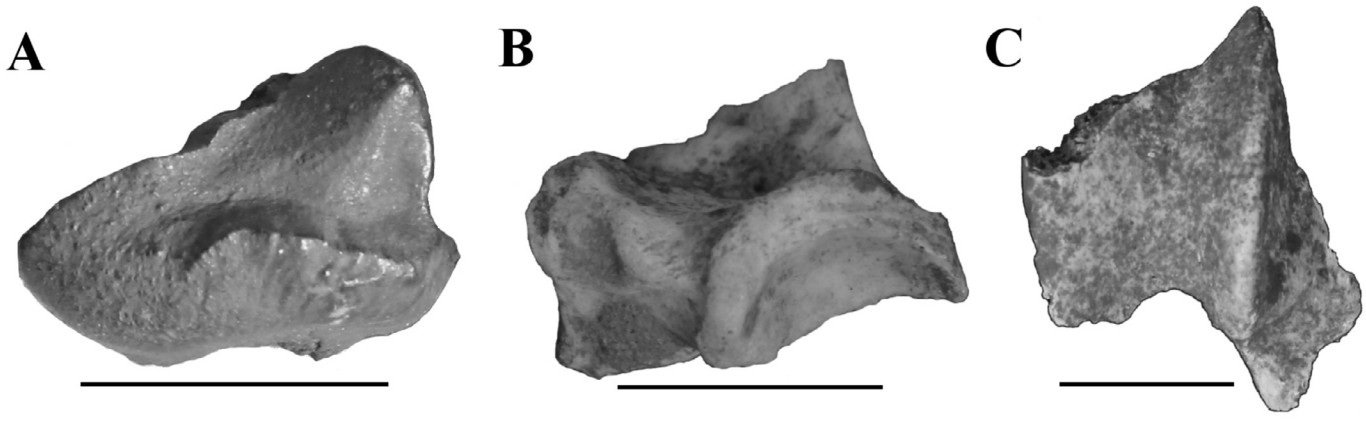

Figure 2. Fossil Carnivora from Gondolin GD 2*. **A**, Partial molar crown (UW87-692) of a medium to large hyaenid. **B**, zygapophysis of thoracic vertebra (UW87-1871) of a medium canid and **C**, right astragalus (UW87-1684) of a medium canid. All scale bars are 1 cm.

Table 1. Taxonomic composition of the Gondolin GD 2* faunal assemblage. The minimum number of juvenile individuals is indicated in brackets.

Order	Family/Tribe	Species	NISP	MNI
CARNIVORA	**Hyaenidae**	Gen. et sp. indet. (large)	1	1
	Canidae	Gen. et sp. indet. (medium)	2	1
	Carnivora indet.		3	–
CETARTIODACTYLA	**Bovidae**			
	Alcelaphini	*Alcelaphus* cf. *buselaphus*	1	1
		Connochaetes sp.	1	1
		Damaliscus sp.	3	1
		Alcelaphini indet.	5	–
	Antilopini	*Antidorcas* sp.	1	1
	Neotragini	indet.	1	1
	Hippotragini	indet.	2	1
	Reduncini	*Redunca arundinum*	13	3
		Redunca fulvorufula	5	3 (1)
		Redunca sp.	10	–
	Tragelaphini	*Tragelaphus* sp.	1	1
		Tragelaphini indet.	1	(1)
	Bovidae indet.	Class I	228	6 (1)
		Class II	386	– (1)
		Class III	48	– (1)
		Class IV	3	1
		Indeterminate class	38	–
		Total bovids	**747**	**23**
	Suidae	*Metridiochoerus andrewsi*	2	1
		Gen. et sp. indet.	2	–
	Cetartiodactyla	indet.	25	–
PERISSODACTYLA	**Equidae**	*Equus* sp	4	2 (1)
HYRACOIDEA	**Procaviidae**	*Procavia* sp.	3	2
LAGOMORPHA	**Leporidae**	Gen. et sp. indet.	3	2 (1)
RODENTIA	**Hystricidae**	*Hystrix makapanensis*	74	2 (1)
		Hystrix africaeaustralis	23	2 (1)
	Pedetidae	*Pedetes capensis*	1	1
MAMMALIA	Indet.	Small	64	–
		Medium	155	–
		Large	18	–
		indet.	121	–
TESTUDINES	**Testudinidae**	indet.		
SQUAMATA		Squamata gen. et sp. indet.	1	1
AVES	**Tytonidae**	*Tyto alba*	1	1
		Aves gen. et sp. indet.	1	1
Indet. faunal remains			10 289	–
Grand total			11 542	40

Description: UW87-1871 is a zygapophysis portion of the thoracic vertebra of a medium-sized canid. UW87-1684 is a right astragalus fragment of a medium-sized canid. The fragmented nature of both specimens prevents any further taxonomic identification.

Carnivora gen. et sp. indet.

Referred specimens: rib tubercle (UW87-223); medial fibula shaft (UW87-1877), canine tooth root (UW87-2218).

Description: UW87-223 is a rib tubercle portion of medium-sized carnivore. UW87-1877 is a medial fibula shaft of a medium-sized carnivore. UW87-2218 is a canine tooth root of a medium-sized carnivore that is partially embedded in breccia. The fragmented and isolated nature of these specimens prevents any further taxonomic identification.

ORDER CETARTIODACTYLA Montgelard *et al*., 1997
Family BOVIDAE Gray, 1821
Tribe ALCELAPHINI de Rochebrune, 1883
Genus ALCELAPHUS Blainville, 1816
Type species *Alcelaphus buselaphus* Pallas, 1766

Alcelaphus* cf. *buselaphus

Referred specimen**:** partial right maxillary second molar (UW87-788; Fig. 3A).

Description**:** unworn molar crown. The tooth size and configuration of the anterior central island, particularly the anterior pinch, which is unique to the tribe, is most similar to *Alcelaphus buselaphus*.

Genus CONNOCHAETES Lichtenstein, 1814
Type species *Connochaetes gnou* Zimmermann, 1780

***Connochaetes* sp.**

Referred specimen: right maxillary second molar (UW87-1861; Fig. 3B).

Description: well-preserved molar crown that is missing a portion of the anterior lobe. We base our identification to genus on the central cavities, which are extended buccally and pinched lingually on both lobes, as well as on the prominent meso- and metastyles.

Genus DAMALISCUS Sclater and Thomas, 1894
Type species *Damaliscus dorcas* Pallas, 1766

***Damaliscus* sp.**

Referred specimens**:** partial maxillary right second molar (UW87-2126; Fig. 3C); partial mandibular right third molar (UW87-2077; Fig. 3D); partial mandibular right third molar (UW87-534).

Description: UW87-2077 is a well-preserved, unworn molar crown. The prominent, lingually projecting central cavities and the mesiodistal size is comparable to *Damaliscus* sp.. Specimen UW87-2126 preserves only the central cavity and surrounding dentine of the anterior lobe. Specimen UW87-534 preserves only the metaconid, the parastylid and a partial root. We base our identification to genus level on the configuration of the central cavity.

Alcelaphini gen. et sp. indet.

Referred specimens**:** partial maxillary second molar (UW87-771); complete mandibular right first molar (UW87-801); partial molar (UW87-1903); partial molar (UW87-1390A); partial molar (UW87-746).

Description**:** the five isolated molars and molar fragments that were assigned to Alcelaphini could not be attributed to either genus or species level due to fragmentation and occlusal wear. Specimen UW87-1903 only preserves the anterior lobe. Specimen UW87-771 only preserves the anterior central cavity with surrounding dentine. Specimen UW87-801 has a high degree of occlusal wear, indicating that it belongs to an old individual. Specimen UW87-1390A only preserves a partial lobe. UW87-746 is an fragmented specimen that preserves a single lobe with a parastylid and an intact goat fold.

Tribe ANTILOPINI Gray, 1821
Genus ANTIDORCAS Sundevall, 1847
Type species *Antidorcas marsupialis* Zimmerman, 1780

***Antidorcas* sp.**

Referred specimen**:** near complete left mandibular fourth premolar (UW87-716; Fig. 3E).

Description: near complete premolar with the anterior root missing. The high state of occlusal wear has obliterated most features but the general shape identifies it as *Antidorcas* sp.

Tribe NEOTRAGINI Sclater and Thomas, 1894

Neotragini gen. et. sp. indet.

Referred specimen**:** left mandibular third molar (UW87-506, Fig. 3F).

Description**:** well-preserved molar without the anterior root. It is highly worn, which obliterated the central island. Based on the angles and size of the lobes, it can be attributed to the tribe Neotragini.

Tribe HIPPOTRAGINI Retzius and Lovén, 1845

Hippotragini gen. et. sp. indet.

Referred specimen**:** partial left mandibular third premolar (UW8-2069; Fig. 3G); partial maxillary molar (UW87-742; Fig. 3H).

Description: UW8-2069 preserves the hypoconid, protoconid and entoconid in addition to the posterior root, while the anterior root, metaconid and paraconid are absent. The general morphology identifies it as Hippotragini, comparatively smaller than *Hippotragus niger*. UW87-742 is a partial specimen; the occlusal surface is highly worn to the point where most features have been lost. The shape of the central cavities and the mesiodistal size is comparable to Hippotragini.

Tribe REDUNCINI Lydekker and Blaine, 1914
Genus REDUNCA C.H. Smith, 1827
Type species *Redunca redunca* Pallas, 1767

Redunca arundinum Boddaert, 1785

Referred specimens: partial left mandibular first molar (UW87-136); partial right mandibular first molar (UW87-497); two partial left maxillary molars (UW87-750, UW87-764); partial right maxillary second molar (UW87-815); partial left mandibular second molar (UW87-1379); partial left maxilla with first and second molars (UW87-2022; Fig. 3I); partial right mandibular third molar (UW87-1751; Fig. 3J); complete right maxillary third molar (UW87-1844); complete right mandibular third molar (UW87-1856); partial left maxillary third premolar (UW87-2044); complete left maxillary second molar (UW87-2047A); partial mandibular third molar (UW87-2098); partial left mandibular second molar (UW87-695).

Description: the presence of basal pillars, parastyles, as well as the shape of the molar lobes identify this specimen as *Redunca arundinum*. The lower molars of *R. arundinum* preserve goat folds, while the upper molars preserve prominent mesostyles and a lingually pinched central cavity. Only the upper third molar has two lobes and does not display the lingually pinched island of the upper first and second molars. Specimens UW87-1844, UW87-1751 and UW87-136 are well-preserved molar crowns. Specimen UW87-497 is a well-preserved molar, with the anterior root missing. Specimen UW87-2098 preserves only the posterior lobe (entoconid, hypoconid and hypoconulid). UW87-1379 is a partial specimen (roots, lingual enamel and metastyle absent). Specimens UW87-750 and UW87-764 are parts of the same molar that is broken buccolingually between the two lobes. For both specimens, the roots and the buccal enamel are absent. Specimen UW87-815 is missing the roots and buccal enamel and it is completely covered in manganese. Specimen UW87-750 makes up the posterior lobe and lingual

enamel; UW87-764 makes up the anterior lobe, including central cavity. Specimen UW87-695 preserves only the anterior lobe with the parastylid, goat fold and basal pillar intact. The left upper premolar UW87-2044 is well preserved but the buccal roots are absent. The metacone is thin/reduced. The sharply pointed metastyle, prominent rib and shape of the central cavity identifies it as *R. arundinum*. UW87-2022 is a partial left maxilla with intact upper first and second molars and an empty socket for the fourth premolar preserved (Fig. 3I). The maxilla is fractured along the alveolar ridges between the second and third molars and between the third and fourth premolars. Based on differences in state of occlusal wear and multiples of the same elements, we estimate that the assemblage has at least three adult *R. arundinum* individuals.

Redunca fulvorufula Afzelius, 1815

Referred specimens: partial left mandibular second molar (UW87-811; Fig. 3K); near complete right mandibular third premolar (UW87-532; Fig. 3L); near complete left mandibular fourth premolar (UW87-1752; Fig. 3M); right mandible with first molar (UW87-2204; Fig. 3N); near complete left maxillary second molar (UW87-1823).

Description: the presence of the basal pillars, parastylids and the shape of the central cavities identify the molars as *Redunca fulvorufula*. The central cavities are pinched lingually on the posterior lobes of the upper molars, while the lower molars display no pinching. UW87-811 is a worn molar without the anterior root. The lower third (UW87-532) and fourth (UW87-1752) premolar crowns are both worn. The shape and morphology of the premolars identified them as *R. fulvorufula*. Specimen UW87-1823 is missing parts of the posterior and anterior roots. The mandible (UW87-2204) is incomplete, broken off distally to the foramen and at the alveolar region that holds the second and third molars. It preserves a complete, unworn first molar and the empty alveolar sockets for the third and fourth premolars. The different stages of wearing and tooth eruption indicate that the sample comprises at least one juvenile, one prime adult and one old adult.

***Redunca* sp.**

Referred specimens: near complete left mandibular third premolar (UW87-499); partial left maxillary second molar (UW87-681); near complete right maxillary third premolar (UW87-691); partial right maxillary first molar (UW87-708); partial left maxillary first or second molar (UW87-2109); incomplete molar (UW87-509A); partial molar (UW87-806A); partial molar (UW87-806B); maxillary left second molar (UW87-693); partial left mandibular third molar (UW87-2098).

Description: UW87-499 is highly worn and the posterior root is absent. The shape and general morphology identify it as *Redunca* sp., but the highly worn occlusal features prevent specific identification. UW87-2109 is missing the lingual enamel, basal pillar and roots. UW87-691 is a well-preserved premolar crown. Specimen UW87-708 is highly worn and missing the anterior root. UW87-681 is a partial specimen that preserves only the posterior lobe. Specimens UW87-509A and UW87-806A preserve only the central cavity and surrounding dentine. Specimen UW87-806B preserves only the anterior lobe. Specimen UW87-693 only preserves the anterior lobe. UW87-2098 is a partial molar crown.

Tribe TRAGELAPHINI Blyth, 1863
Genus TRAGELAPHUS de Blainville, 1816
Type species *Tragelaphus scriptus* Pallas, 1766

***Tragelaphus* sp.**

Referred specimen**:** near complete left maxillary fourth premolar (UW87-498; Fig. 3O).

Description: the premolar preserves the crown only. The general morphology of the tooth and shape of the central island identifies it as *Tragelaphus* sp.

Tragelaphini gen et. sp. indet.

Referred specimen**:** partial left mandibular second molar (UW87-741; Fig. 3P).

Description: the molar is missing the distal lobe and the crown is unworn. The shape of the lobe and the buccal-lingual distance are characteristic of Tragelaphini. It belongs to a young adult individual.

Family SUIDAE Gray, 1821
Tribe PHACOCHOERINI Gray, 1868
Genus METRIDIOCHOERUS Hopwood, 1926

Metridiochoerus andrewsi Hopwood, 1926

Referred specimens**:** partial right mandibular second molar (UW87-500; Fig. 4A,B); partial left maxillary second molar (UW87-752; Fig. 4C)

Description: these two molars belong to the extinct species *Metridiochoerus andrewsi*. The left upper second molar (UW87 752) has distinct pillars but is a partial specimen, with only the crown preserved. It possibly belongs to a juvenile *M. andrewsi*. The right lower second premolar (UW87-500) only preserves the posterior portion with a moderate to heavy wear pattern. There is a combination of pillars and continuous enamel folds.

Suidae gen. et sp. indet.

Referred specimens: partial maxillary molar (UW87-761; Fig. 4D,E); fragment of canine (UW87-704).

Description: specimen UW87-761 is a highly worn molar with one of the roots absent. Due to the extensive wear, it is impossible to identify the side or which particular molar it is. The UW87-704 has parallel striations that are similar to the enamel found on suid canines.

ORDER PERISSODACTYLA Owen, 1848
Family EQUIDAE Gray, 1821
Genus EQUUS Linnaeus, 1758
Tribe EQUINI Gray, 1821
Type species *Equus caballus* Linnaeus, 1758

***Equus* sp.**

Referred specimens: partial deciduous maxillary incisor (UW87-505, Fig. 5A,B); partial cervical vertebra (UW87-

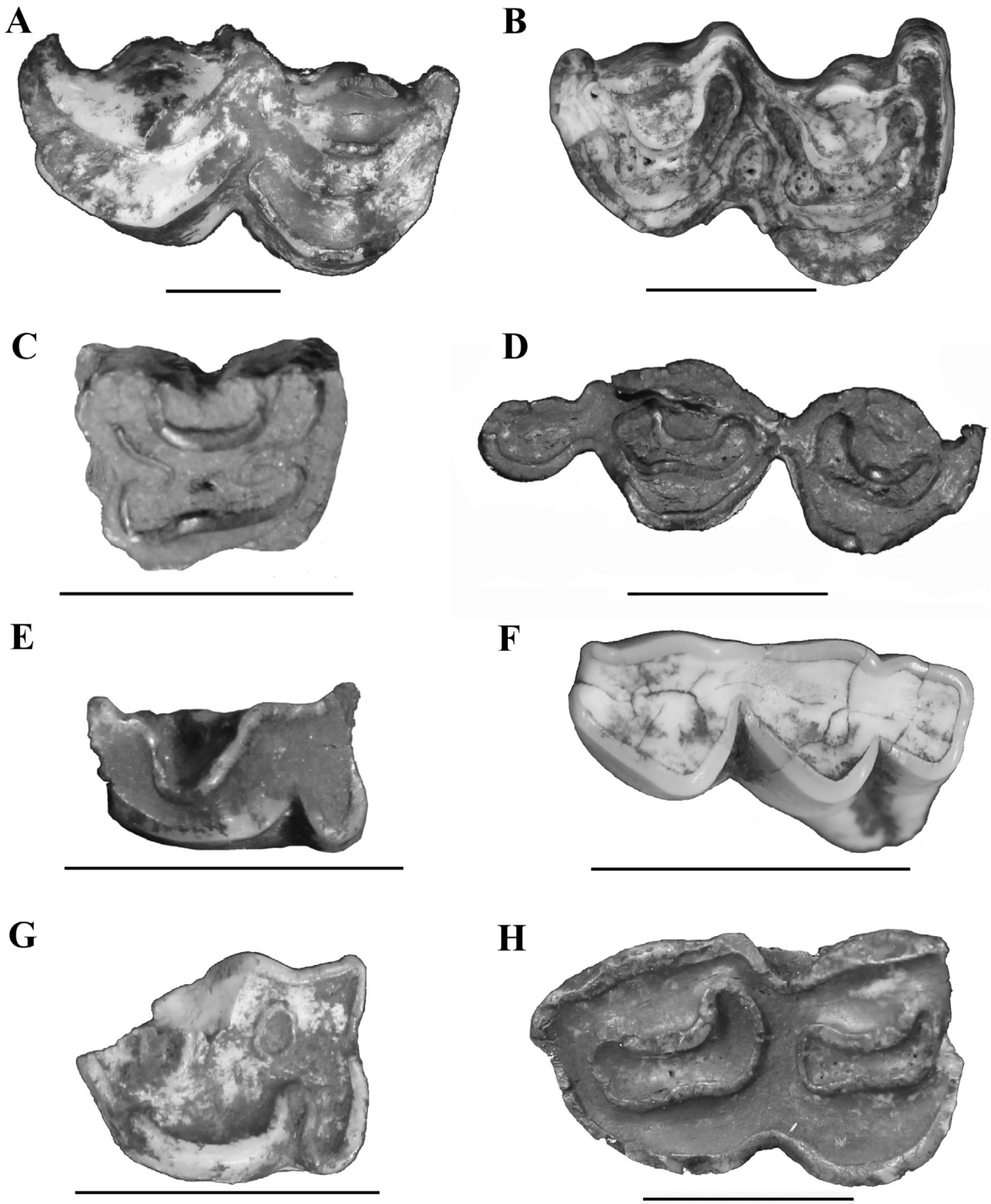

Figure 3. Fossil Bovidae teeth from Gondolin GD 2*, all in occlusal view. **A**, *Alcelaphus* cf. *buselaphus* right M^2 (UW87-788); **B**, *Connochaetes* sp. right M^2 (UW87-1861); **C**, *Damaliscus* sp. right M^2 (UW87-2126). **D**, *Damaliscus* sp. right M_3 (UW87-2077); **E**, *Antidorcas* sp. left PM_4 (UW87-716); **F**, Neotragini indet. left M_3 (UW87-506); **G**, Hippotragini indet. right PM_2 (UW87-2069); **H**, Hippotragini indet. molar (UW87-742). All scale bars are 1 cm.

Continued on p. 100

1560; Fig 5C); right proximal metacarpal (UW87-2203; Fig. 5D); fragment of axis (UW87-1287 Fig. 5E)

Description: the incisor is comparable in size to specimen M196, a deciduous incisor from Makapansgat that belongs to the extinct three-toed horse *Hipparion*. However, because it is a deciduous incisor, we consider that a taxonomic identification based on dimensions only is not secure and we prefer to assign this specimen to an indeterminable equid. The fragments of the transverse processes of an axis and a cervical vertebra closely resemble *Equus* sp. in shape, size and morphology. The metacarpal (UW87-2203) preserves only the lateral proximal epiphysis and shaft. This specimen belongs to an adult, based on the epiphyseal fusion state of the bone.

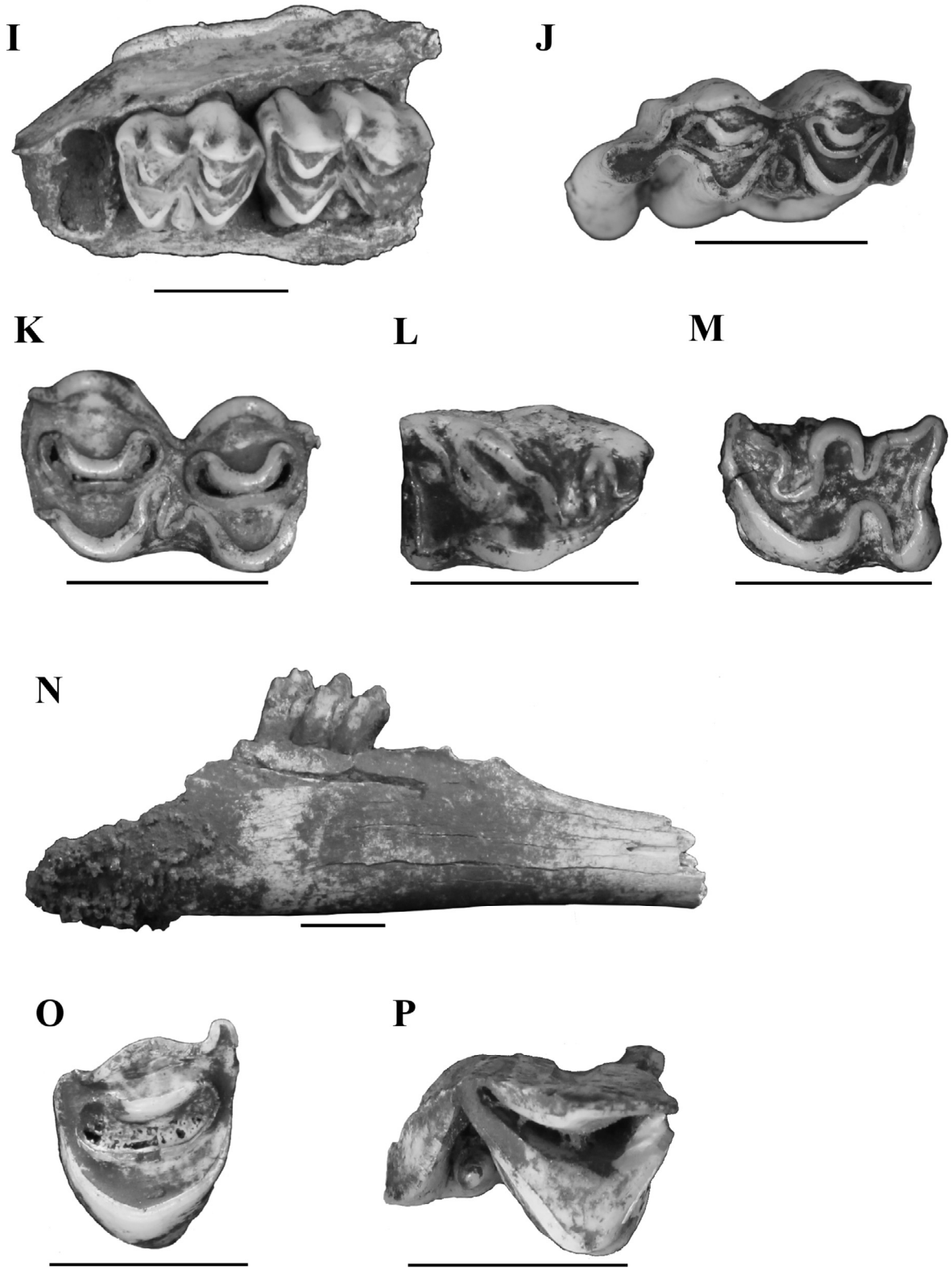

Figure 3 (*continued*). **I**, *Redunca arundinum* left maxilla (UW87-2022); **J**, *R. arundinum* right M_3 (UW87-1751); **K**, *R. fulvorufula* left M_2 (UW87-811); **L**, *R. fulvorufula* right PM_3 (UW87-532); **M**, *R. fulvorufula* left PM_4 (UW87-1752); **N**, *R. fulvorufula* right mandible with M_1 (UW87-2204); **O**, *Tragelaphus* sp. left PM^4 (UW87-498); **P**, Tragelaphini indet. left M_2 (UW87-741). All scale bars are 1 cm.

ORDER HYRACOIDEA Huxley, 1869
Family PROCAVIIDAE Thomas, 1892
Genus PROCAVIA Storr, 1780
Type species *Procavia capensis* Storr, 1780

***Procavia* sp.**

Referred specimens: partial upper left first molar (UW87-751); partial left first incisor (UW87-537); left distal humerus (UW87-2107).

Description: the molar preserves only the crown. It is smaller than *Procavia transvaalensis*; the shape and overall morphology is similar to an adult *P. capensis* but it was not possible to distinguish from *P. antiqua* because complete cusps are not preserved. UW87-537 is worn on the lingual

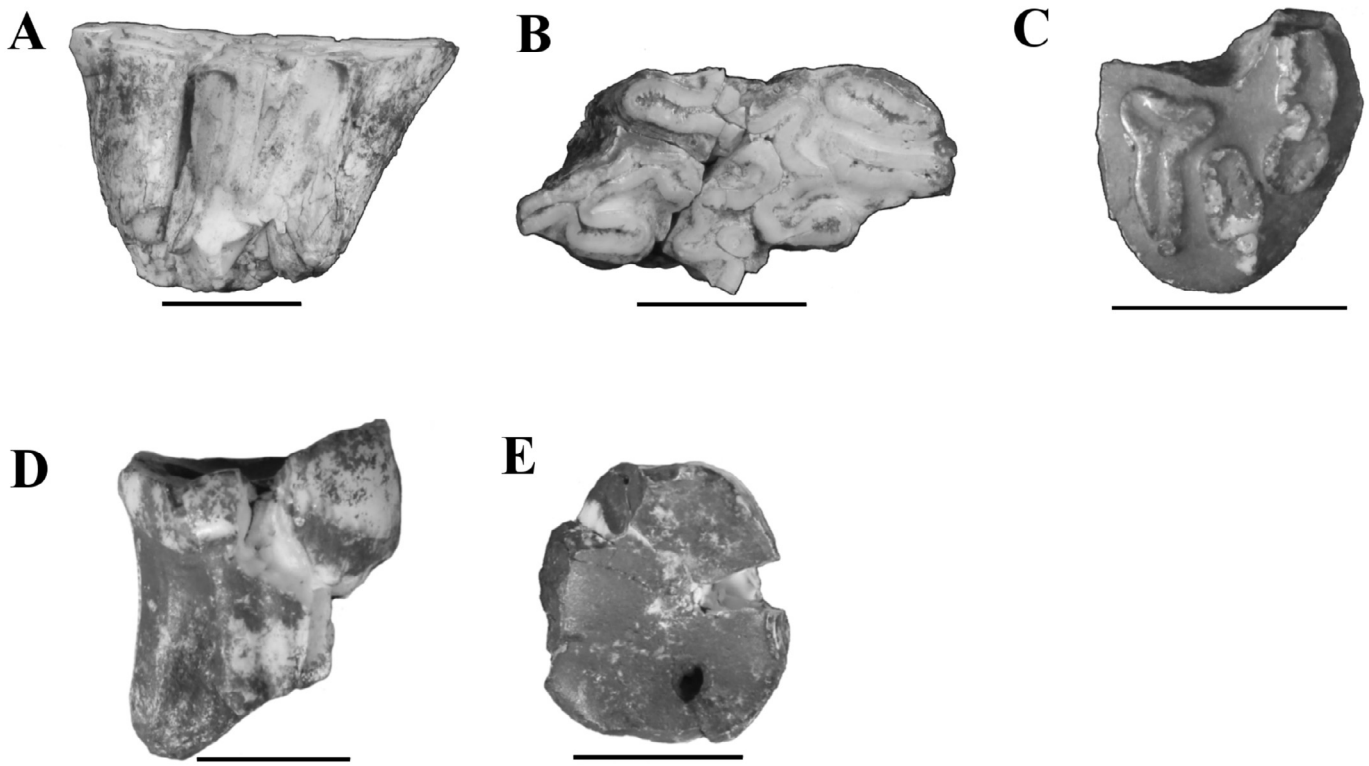

Figure 4. Fossil Suidae from Gondolin GD 2*. **A**, *Metridiochoerus andrewsi* lateral view and **B**, occlusal view of right M2 (UW87-500); **C**, *M. andrewsi* left M^2 (UW87-752); **D**, Suidae gen. et sp. indet. lateral view and **E**, occlusal view of upper molar (UW87-761). All scale bars are 1 cm.

side where it occludes to the lower incisor. It is a partial specimen and we could not determine the age of the individual. The distal humerus (UW87-2107) has a fused epiphysis, indicating that the individual is an adult. Based on the dimensions this specimen, we can exclude *P. transvaalensis* but we cannot distinguish between the extant species *P. capensis* and the extinct species *P. antiqua*.

ORDER LAGOMORPHA Brandt, 1855
Family LEPORIDAE Fischer von Waldheim, 1817

Leporidae gen. et sp. indet.

Referred specimens: proximal left tibia (UW87-1906); distal right femur (UW87-1888); distal left humerus (UW87-2033).

Description: the small sample size and incomplete nature of the specimens makes further taxonomic classification impossible. The proximal tibia and distal humerus both have fused epiphyses, while the distal femur is not fused, indicating that it belongs to a juvenile individual.

ORDER RODENTIA Bowdich, 1821
Family HYSTRICIDAE Fischer von Waldheim, 1817
Genus HYSTRIX Linnaeus, 1758
Type species *Hystrix cristata* Linnaeus, 1758

Hystrix africaeaustralis Peters 1852

Referred specimens: Table 2 provides a summary of the sample of 11 postcranial and 12 dental remains assigned to this species.

Description: right astragalus of a juvenile (Fig. 6C), nine phalanges (e.g. Fig. 6D) and eight molars represent the major skeletal parts of *H. africaeaustralis* recovered from GD 2*. These remains belong to one adult and one juvenile *H. africaeaustralis*.

Hystrix makapanensis Greenwood, 1958

Referred specimens: Table 2 lists the 74 new specimens from GD 2* identified as *H. makapanensis*.

Description: these specimens include eight craniodental and 66 postcranial remains, representing at least one adult and one juvenile. The postcranial material generally resembles the extant species *H. africaeaustralis*, but the remains are about 1.5 times larger. Comparison of the material to known *H. makapanensis* remains from Gondolin confirmed the taxonomic assignement of the specimens (Maguire 1976; Adams 2012b; GD 2 assemblage at Ditsong National Museum of Natural History in Pretoria). Of importance are the right distal humerus (UW87-254) and a right maxilla (UW87-1810; Fig. 6B) of an adult individual of *H. makapanensis*. The maxilla preserves three complete molars.

Family PEDETIDAE Gray, 1825
Genus PEDETES Illiger, 1811

Pedetes capensis Forster, 1778

Referred specimens: partial molar (UW87-728)

Description: the molar is morphologically identical to modern specimens and we confidently attribute it to *P. capensis*. Because it is a partial specimen, we could not estimate the age of the individual.

Mortality profiles

Class I bovids are represented by one juvenile, five adults and one old adult. Class II bovids are represented

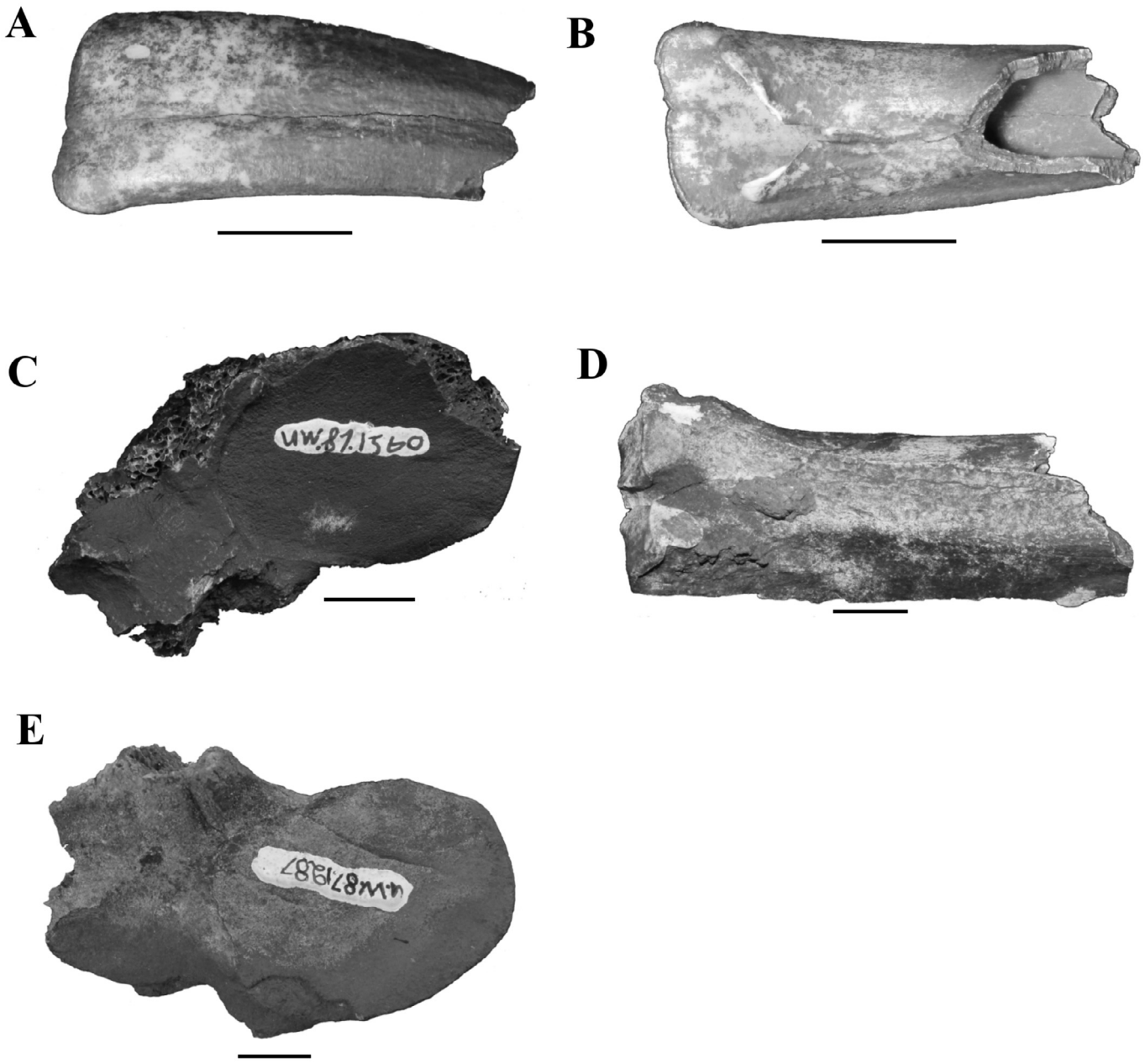

Figure 5. Fossil Equidae from Gondolin GD 2*. **A**, *Equus* sp. buccal view and **B**, lingual view of deciduous first incisor (UW87-505); **C**, *Equus* sp. transverse process of a cervical vertebra (UW87-1560); **D**, *Equus* sp. right lateral proximal metacarpal (UW87-2203); **E**, *Equus* sp. transverse process of axis (UW87-1287). All scale bars are 1 cm.

by two juveniles, four adults and two old adults. Class III bovids are represented by two juveniles and five adults. There is only one size class IV bovid represented in the assemblage by three worn, incomplete teeth, indicating an old individual. Figure 7 combines the MNI per age category for size classes I, II and III bovids, for which sample sizes are large enough to propose some interpretations. The mortality profiles for these three size classes are closer to catastrophic mortality patterns, with prime adults dominating.

Both species of porcupines are represented by two individuals each, with an adult and a juvenile in each case. The leporid remains belong to one adult and one juvenile. The single *Pedetes capensis* specimen could not be assigned a specific age. The *Procavia* material represents the remains of at least one adult individual.

Bone fragmentation

Only 241 of the 11 542 bones (1.9%) studied are complete bones, indicating a high rate of fragmentation. Complete bones consist primarily of phalanges and compact bones such as carpals, tarsals, and sesamoids. No articulated, associated or antimeric sets of bones were recovered. Figure 8 presents the distribution of the 10 289 unidentifiable bone fragments according to size categories. The majority of the bone fragments (79.7%) in the assemblage are ≤2.9 cm in size. The fragmentation ratio is 10.9.

Table 3 summarizes the fracture features coded for the long bone fragments. We recorded features consistent both with dry and green breakages, with a larger sample of long bones with smooth (53.3%) and curved or V-shaped fractures (83.3%). This indicates that breakage of long bones occurred at an early stage in the accumula-

Table 2. NISP, MNE, MAU and %MAU values for the *Hystrix makapanensis* and *H. africaeaustralis* material from GD 2*.

Taxon:	*Hystrix makapanensis*				*Hystrix africaeaustralis*			
Element	NISP	MNE	MAU	%MAU	NISP	MNE	MAU	%MAU
Mandible	–	–	–	–	1	1	0.25	100
Maxilla	1	1	0.25	50	–	–	–	–
Upper molar	3	3	0.25	50	2	2	0.17	67
Lower molar	4	4	0.33	67	3	3	0.25	100
Molar indet.	–	–	–	–	3	3	–	–
Deciduous tooth	–	–	–	–	1*	1	–	–
Incisor	–	–	–	–	2	2	0.25	100
Axis	1	1	0.5	100	–	–	–	–
Humerus	2	1	0.25	50	–	–	–	–
Radius	1	1	0.25	50	–	–	–	–
Ulna	2	2	0.5	100	–	–	–	–
Femur	1*	1	0.25	50	–	–	–	–
Tibia	–	–	–	–	1	1	0.25	100
Calcaneus	1	1	0.25	50	–	–	–	–
Astragalus	1	1	0.25	50	1*	1	0.25	100
Metacarpals	8*	8	0.4	80	–	–	–	–
Metatarsals	2	2	0.1	20	–	–	–	–
Metapodial indet.	5*	5	0.6	63	–	–	–	–
Metapodial total	15	15	0.38	75	–	–	–	–
Cuneiform	2*	2	0.5	100	–	–	–	–
Cuboid	1	1	0.25	50	–	–	–	–
Proximal phalanx	10	10	0.25	50	1	1	0.02	10
Medial phalanx	17	16	0.5	100	1	1	0.03	12
Distal phalanx	12	12	0.3	60	4	4	0.1	40
Phalanx indet.	–	–	–	–	3	3	–	–

*Specimens attributed to a juvenile individual.

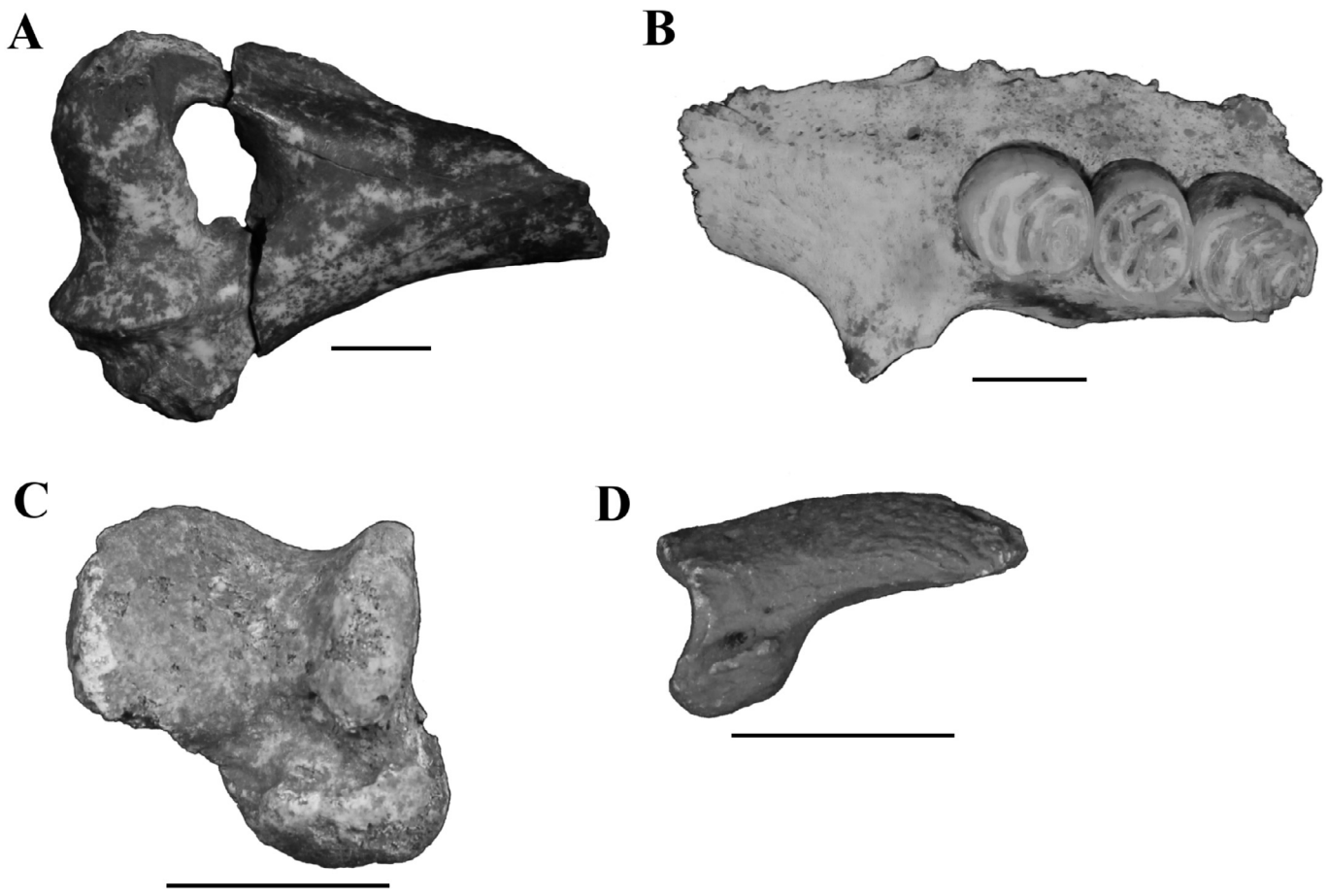

Figure 6. Fossil *Hystrix makapanensis* and *Hystrix africaeaustralis* remains from Gondolin GD 2*. **A**, *H. makapanensis* right distal humerus (UW87-254); **B**, *H. makapanensis* right maxilla (UW87-1810); **C**, juvenile *H. africaeaustralis* right astragalus, dorsal view (UW87-241); **D**, *H. makapanensis* distal phalanx (UW87-349). All scale bars are 1 cm.

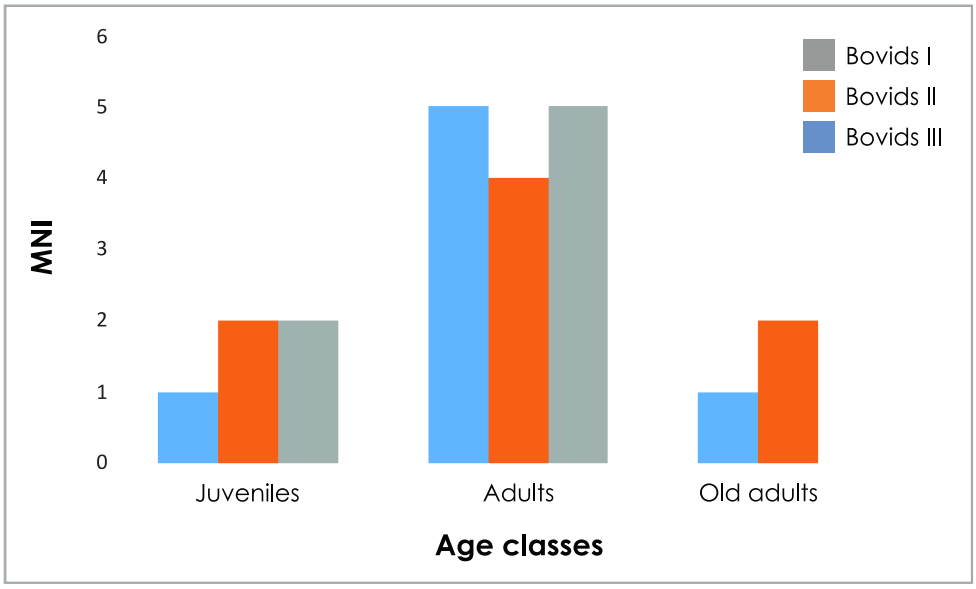

Figure 7. Mortality profiles for the size classes I, II and III bovids. Data in MNI per age class.

tion of the faunal assemblage, when most of the bones were still fresh. Several specimens display both dry and green fracture attributes. Only 12.2% of the shafts preserve their complete circumference. There is no bone cylinders and long bones tend to be represented mostly by their proximal and/or distal epiphyses (see below).

Table 3. Long bone breakage patterns for the GD 2* assemblage (data in NISP).

Category	Description		
Fracture angle	oblique 75	right 103	oblique & right 19
Fracture outline	curved/V-shaped 164	transverse 49	intermediate 17
Fracture edge	smooth 105	jagged 79	smooth & jagged 13
Circumference	<50% 167	>50% 6	complete 24

Skeletal part representation

We estimated the skeletal element representation for small and medium bovids (size classes I and II) using %MAU values (Tables 4 and 5). The best-preserved elements are compact bones, including tarsals, carpals and patellae, alongside phalanges and the distal and/or proximal epiphyses of long bones from the upper and lower limbs. Long bone shafts, ribs and vertebrae are under-represented. Some fragile elements such as hyoid bones and juvenile skeletal remains are also present. Larger bovids (size classes III and IV) are only represented by craniodental material.

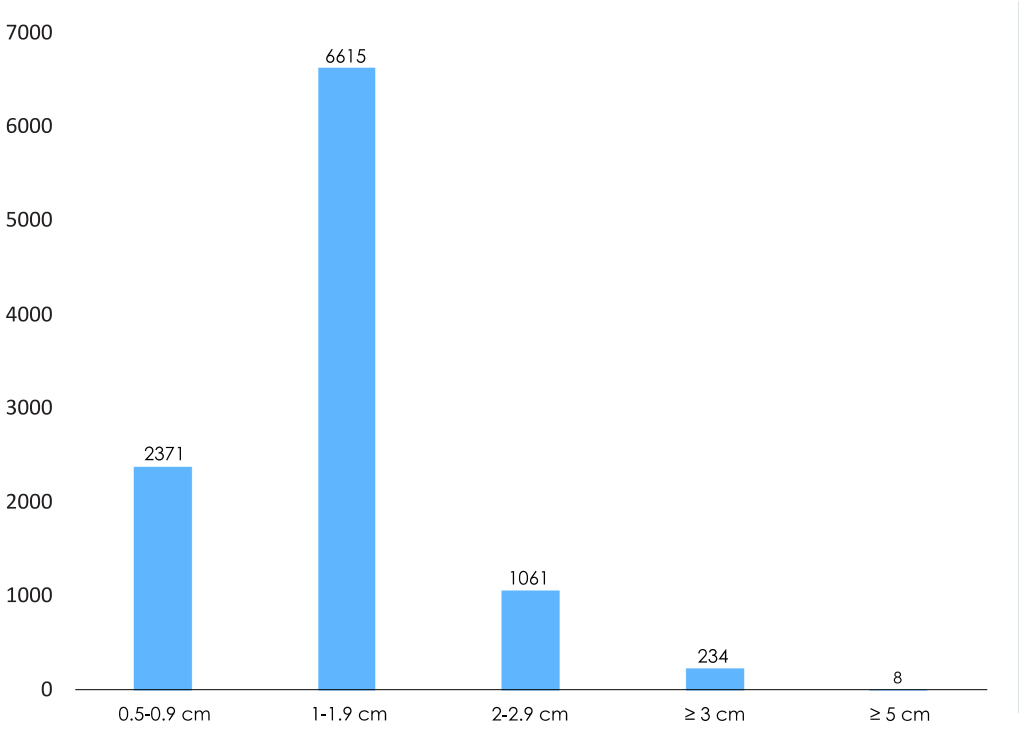

Figure 8. Distribution of unidentifiable bone fragments across size categories.

We produced a scatterplot of $\log_{10}$ transformed %MAU values for the size classes I and II bovids, as well as for *H. makapanensis* remains, against element-specific bone mineral density (BMD) values. For size class I bovids, there is a negative and statistically significant correlation between BMD and element survivorship ($P = 0.04$; $R^2 = 0.09$). For the size class II bovids, there is no statistically significant correlation between the abundance of skeletal parts and bone density ($P = 0.68$; $R^2 = 0.04$). No correlation was found between *H. makapanensis* and BMD ($p = 0.96$; $R^2 = 0.00009$).

Fluvial transport

The bovid material (size classes I–III) was placed into the five Voorhies Groups (Fig. 9). Almost all groups are well-represented, except for the ramus of the mandible (Group II & III), which is absent from the assemblage. Material from the lag group (mandibular bodies and cranial material) is as well represented as the material that is easily transported (ribs, vertebrae and sacrum). Only fifteen elements in the assemblage (0.9%) exhibit signs of polishing consistent with abrasion caused during transport in a body of water.

Table 4. NISP, MNE, MAU and %MAU values for size class I bovid postcranial material from GD 2*.

Element	NISP	MNE	MAU	%MAU
Astragalus	7	7	3.50	100.00
Humerus distal	7	6	3.00	85.71
Lateral malleolus	6	6	3.00	85.71
External cuneiform	6	6	3.00	85.71
Intermediate phalanx proximal	22	22	2.75	78.57
Intermediate phalanx distal	21	21	2.63	75.00
Radius proximal	5	5	2.50	71.43
Femur proximal	5	5	2.50	71.43
Pelvis (acetabulum)	5	5	2.50	71.43
Lunate	5	5	2.50	71.43
Third phalanx	18	18	2.25	64.29
Cuneiform	4	4	2.00	57.14
Magnum	4	4	2.00	57.14
Cubonavicular	4	4	2.00	57.14
Metacarpal proximal	3	3	1.50	42.86
Scaphoid	3	3	1.50	42.86
Unciform	3	3	1.50	42.86
Femur distal	3	3	1.50	42.86
First phalanx distal	12	12	1.50	42.86
First phalanx proximal	11	11	1.37	39.29
Proximal sesamoid	19	19	1.19	33.93
First phalanx shaft	9	9	1.13	32.14
Metapodial condyle	9	9	1.13	32.14
Humerus proximal	2	2	1.00	28.57
Patella	2	2	1.00	28.57
Calcaneum	2	2	1.00	28.57
Metatarsal proximal	2	2	1.00	28.57
Hyoid	1	1	1.00	28.57
Thoracic vertebra	11	11	0.92	26.19
Lumbar vertebra	4	4	0.80	22.86
Metacarpal shaft	1	1	0.50	14.29
Pisiform	1	1	0.50	14.29
Radius distal	1	1	0.50	14.29
Metatarsal shaft	1	1	0.50	14.29
Tibia proximal	1	1	0.50	14.29
Tibia shaft	1	1	0.50	14.29
Ulna distal	1	1	0.50	14.29
Distal sesamoid	4	4	0.50	14.29
Cervical vertebra	3	3	0.43	12.24
Caudal vertebra	2	2	0.20	5.71
Rib proximal	5	5	0.19	5.49
Splints	1	1	0.13	3.57
Rib shaft	3	3	0.10	3.30
Scapula	0	0	0	0
Humerus shaft	0	0	0	0
Radius shaft	0	0	0	0
Ulna shaft	0	0	0	0
Ulna proximal	0	0	0	0
Metarcarpal distal	0	0	0	0
Femur shaft	0	0	0	0
Tibia distal	0	0	0	0
Metatarsal distal	0	0	0	0

Table 5. NISP, MNE, MAU and %MAU values for size class II bovid postcranial material from GD 2*.

Element	NISP	MNE	MAU	%MAU
Metacarpal proximal	8	8	4.00	100.00
Cubonavicular	8	8	4.00	100.00
Metapodial condyle	28	28	3.50	87.50
Pelvis (acetabulum)	7	7	3.50	87.50
Patella	7	7	3.50	87.50
Lateral malleolus	7	7	3.50	87.50
Ulna proximal	6	6	3.00	75.00
Femur proximal	6	6	3.00	75.00
Femur distal	6	6	3.00	75.00
First phalanx proximal	24	24	3.00	75.00
External cuneiform	6	6	3.00	75.00
Calcaneus	6	6	3.00	75.00
Astragalus	6	5	2.50	62.50
Magnum	5	5	2.50	62.50
Metatarsal proximal	5	5	2.50	62.50
Internal cuneiform	5	5	2.50	62.50
Distal phalanx	18	18	2.25	56.25
Radius distal	4	4	2.00	50.00
Tibia shaft	4	4	2.00	50.00
First phalanx shaft	16	16	2.00	50.00
Cuneiform	4	4	2.00	50.00
Intermediate phalanx distal	14	14	1.75	43.75
Intermediate phalanx proximal	13	13	1.63	40.63
First phalanx distal	12	12	1.50	37.50
Proximal sesamoids	24	24	1.50	37.50
Radius proximal	3	3	1.50	37.50
Scaphoid	3	3	1.50	37.50
Metatarsal distal	2	2	1.00	25.00
Tibia proximal	2	2	1.00	25.00
Metacarpal distal	2	2	1.00	25.00
Tibia distal	2	2	1.00	25.00
Humerus proximal	2	2	1.00	25.00
Unciform	2	2	1.00	25.00
Hyoid	1	1	1.00	25.00
Thoracic vertebra	9	8	0.62	15.38
Humerus shaft	1	1	0.50	12.50
Humerus distal	1	1	0.50	12.50
Metacarpal shaft	1	1	0.50	12.50
Metatarsal shaft	1	1	0.50	12.50
Lunate	1	1	0.50	12.50
Scapula (spine)	1	1	0.50	12.50
Splints	4	4	0.50	12.50
Lumbar vertebra	2	2	0.40	10.00
Distal sesamoids	3	3	0.38	9.38
Rib proximal	8	8	0.31	7.69
Cervical vertebra	2	2	0.29	7.14
Rib shaft	8	8	0.27	6.73
Caudal vertebra	2	2	0.20	5.00
Femur shaft	0	0	0	0
Radius shaft	0	0	0	0
Scapula (glenoid)	0	0	0	0
Scapula (blade)	0	0	0	0

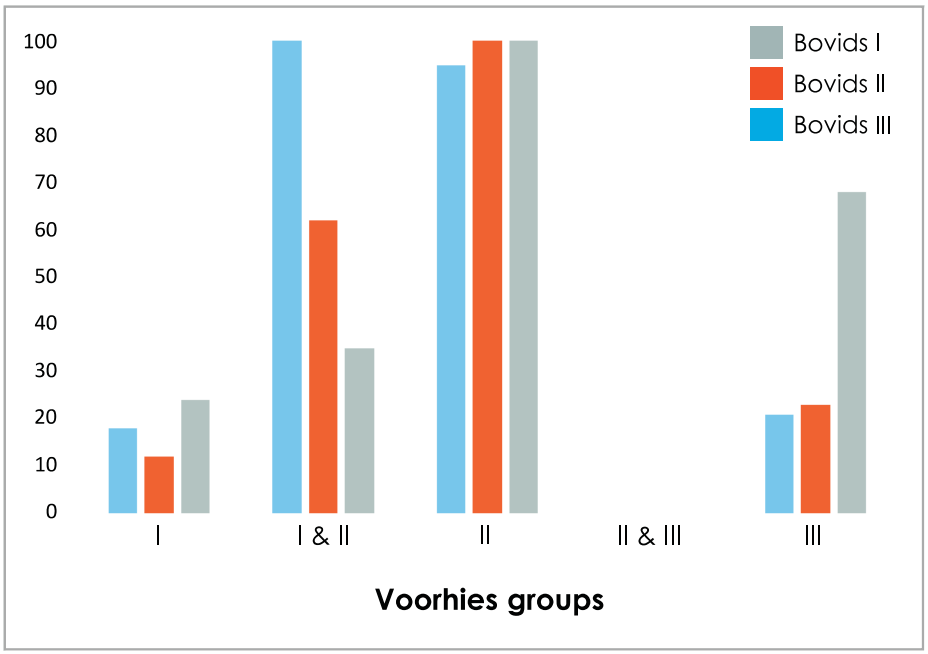

Figure 9. Distribution of total %MAU for bovid size classes I, II and III across the five Voorhies groups.

Bone surface modifications

The sample analysed for bone surface modifications comprises 1617 specimens, which include the 1227 taxonomically identified specimens and 390 unidentifiable bone and long bone shaft fragments that were ≥3 cm in length.

Manganese staining

Manganese dioxide coatings were recorded in varying degrees on each of the 1 617 specimens. The majority of the specimens have a high level of manganese dioxide coating: 75% of the bone fragments exhibit a >50% surface coating; 33% displayed a 50–90% surface coverage and 43% have an intense coating of 90–100% of the specimen surface. The manganese dioxide coatings have certainly hindered our ability to detect all bone surface modifications. This suggests that the traces produced by biotic agents described below only represent a fraction of the actual amount of bone surface modifications and that the quantitative data should be regarded as minimum values.

Weathering

Of the inspected material, 39% of the assemblage display no signs of weathering, while nearly half the assemblage (48%) display the fine longitudinal cracks that characterize weathering stage 1. A small number of specimens (12%) display characteristics attributable to weathering stage 2. Only two specimens present the deep longitudinal cracks, flaking and bone loss that characterize weathering stage 3. No extreme weathering stages (stages 4 and 5) are recorded.

Biotic modifications

We identified 198 specimens that bear evidence of biotic damage produced by rodents, carnivores, plant roots and rootlets, and invertebrates. Table 6 summarizes the numbers and percentages of biotically modified elements by taxonomic grouping. A total of 46 specimens bear evidence of rodent modification, ranging from broad, shallow, parallel scrape marks (34.7%; Fig. 10), gnawed edges (26%) to scooping of cancellous bone (41.3%). Only one specimen shows evidence of both scrape marks and scooping. Rodent gnawing occurs mostly on long bones, where scooping of cancellous bone is recorded. The location and dimensions of most rodent gnawing damage (53%) are consistent with modifications caused by porcupines. Small rodent modifications are visible on long bones and vertebrae. Mammalian carnivore modifications occur on 56 specimens in the form of tooth pits (Fig. 11), gnawed/crenulated edges, and digestive corrosion (Table 7). Carnivore modifications were recorded primarily on bovid remains, and particularly on long bones and patellae. One *H. africaeaustralis* astragalus exhibits signs of digestive corrosion, while a *H. makapanensis* calcaneus has a tooth pit. The dimensions of the carnivore tooth pits are consistent with damage produced during gnawing by medium to large mammalian carnivores. Forty-six specimens (2.9% of the taphonomically

Table 6. Number of biotically modified elements from GD 2* by taxonomic group (data in NISP).

Taxonomic group	Invertebrate modification	Rodent gnawing	Carnivore damage	Root etching
Bovids Class I	17	6	5	5
Bovids Class II	18	13	27	7
Bovids Class III	2	–	6	–
Bovids Indet.	2	1	–	2
Suids	1	–	–	–
Artiodactyla	–	–	–	2
Equids	–	1	–	–
H. makapanensis	7	–	2	–
H. africaeaustralis	1	–	1	1
Mammal indet.	12	15	12	21
Indet. bone fragment	–	2	1	5
Indet. cranial fragment	–	–	–	3
Total	60 (3.7%)	38 (2.4%)	54 (3.3%)	46 (2.9%)

ISSN 2410-4418 *Palaeont. afr.* (2023) **55**: 92–112



Figure 10. Example of porcupine gnawing on the Gondolin GD 2* fossil assemblage. **A**, parallel sets of gnawing marks from rodent incisors on a bovid horn core (UW87-1838), **B**, ×0.67 magnification of the gnawing marks. The scale bars are 1 cm.



Figure 11. Example of carnivore gnawing on the Gondolin GD 2* fossil assemblage: carnivore tooth pits on the outer cortex of a long bone shaft fragment (UW87-298). The scale bar is 1 mm.

analysed assemblage) bear evidence of root acid etching. Sixty specimens were recorded having microscopic pits (85.25%) and pits with striations (14.75%), possibly caused by invertebrates. The pits are all featureless at the base and around the rim, but nine specimens had radiating striations around the rim. These radiating striations are comparable to termite damage as described by Backwell *et al*. (2012). We found no evidence of bird of prey damage (e.g. scores, punctures and notches caused by beak and/or talon impact or light acid etching) in the GD 2* assemblage.

DISCUSSION

Biochronological interpretations for the GD 2* assemblage

The presence of the time-sensitive taxa *M. andrewsi*, *H. makapanensis*, and *Equus* sp. is useful in bracketing the chronological period during which the assemblage accumulated. *M. andrewsi* is known from a number of Late Pliocene and Early Pleistocene sites in South Africa. The oldest occurrences of this species in the southern African region come from Makapansgat Member 3 dated between 3.03 and 2.58 Ma (Harris & White 1979; Herries 2003) and Milo's Pit A from Bolt's Farm, regarded as a Late Pliocene fossil locality (Gommery *et al*. 2012). Its presence is documented from younger deposits dated between 1.9 and 1.5 Ma at Kromdraai A (Pickford 2013a), GD 2 at Gondolin (Adams 2006; Pickford 2013b) and Cooper's D (Berger *et al*. 2003; de Ruiter *et al*. 2009). The identification of *M. andrewsi* inside the GD 2* sample therefore places this deposit in the time bracket of 3.03–1.5 Ma. *Hystrix makapanensis* was first identified in Makapansgat Mem-

Table 7. Carnivore damage on the GD 2* faunal remains. Data presented in number of remains with acid etching and/or gnawing damage (tooth pits and/or crenulated edges).

Element	Bov I	Bov II	Bov III	Mammal	*H. makapanensis*	*H. africaeaustralis*
Axis	0/0	0/0	0/1	0/0	0/0	0/0
Vertebra	0/0	1/0	0/0	1/0	0/0	0/0
Sternebrae	0/0	0/1	0/0	0/0	0/0	0/0
Rib	0/0	0/0	0/0	1/2	0/0	0/0
Humerus	0/1	0/3	0/1	0/0	0/0	0/0
Femur	0/0	0/2	0/1	0/0	0/0	0/0
Tibia	0/1	0/0	0/1	0/0	0/0	0/0
Metapodial	0/0	3/2	0/1	0/0	0/0	0/0
Long bone shaft	0/0	0/0	0/0	4/4	0/0	0/0
Patella	0/1	0/5	0/1	0/0	0/0	0/0
Lateral malleolus	0/0	1/0	0/0	0/0	0/0	0/0
Calcaneum	0/0	1/0	0/0	0/0	0/1	0/0
Astragalus	0/0	0/0	0/0	0/0	0/0	1/1
Cubonavicular	0/1	0/0	0/0	0/0	0/0	0/0
Phalanx	0/1	4/2	0/0	0/0	1/0	1/0
Cuneiform	0/0	1/1	0/0	0/0	0/0	0/0
Total	0/5	11/16	0/6	6/6	1/1	2/1

bers 3 and 4 dated at 3.03–2.58 Ma (Maguire 1976). The only other known occurrence of this species from a South African fossil locality is from GD 2 at Gondolin (Adams 2006, 2012), which has been dated to 1.95–1.78 Ma using faunal correlation and palaeomagnetism (Herries *et al*. 2006). The new *H. makapanensis* material from GD 2* places the deposits within the time bracket from 3.03 to 1.78 Ma.

Four of the specimens recovered from GD 2* belong to the genus *Equus*. The first appearance of *Equus* in East Africa is from the 2.33 Ma Omo Shungura Formation Member G: *Equus oldowayensis* (Hopwood 1937). It is the most widespread and abundant *Equus* species from the Plio-Pleistocene in Ethiopia, Kenya and Tanzania, from beds dated at 2.33–1.0 Ma (Bernor *et al*. 2010). The presence of equid remains in the GD2* assemblage thus provides a maximum age of 2.33 Ma for the deposits.

The combined biochronological data for *M. andrewsi*, *H. makapanensis*, and *Equus* sp. places the GD 2* assemblage in a depositional age bracket of 2.33–1.78 Ma, at the onset of the Pleistocene. This estimate overlaps with the previously estimated dates for GD 2 of 1.95–1.78 Ma (Herries *et al*. 2006).

Small mammal carcasses: accumulation scenarios

Modern porcupines use rocky terrain, crevasses as well as cave systems as habitat and for rearing their young (Estes 1991; Kingdon 1997; Skinner & Chimimba 2005). The GD 2* porcupine assemblage comprises the remains of juvenile *H. africaeaustralis* and *H. makapanensis*, and we have identified gnawing damage attributed to these rodents in the assemblage. This suggests that they may have periodically used the cave. Modern observations document extant red rock hares, springhares and hyraxes thriving in rocky terrain and using caves as habitat (Brain 1981; Estes 1991; Kingdon 1997; Skinner & Chimimba 2005). Based on habitat preferences and ecology of these small mammals, we hypothesize that use of the cave followed by natural death could explain the origin of some of their fossil remains within the GD 2* faunal assemblage. The occurrence of juveniles supports this hypothesis. We exclude avian predators as significant contributors, given the absence of bone damage attributed to birds of prey, the limited percentage of small mammals in the faunal assemblage, and the lack of skeletal part representation consistent with consumption by such predators (Brain 1981; Armstrong & Avery 2014). Medium to large mammalian carnivores, including caracals, jackals and leopards, feed on leporids and hyraxes (e.g. Grobler & Wilson 1972; Brain 1981; Cohen & Kibii 2015). While they could have contributed to accumulate and/or modify some of fossil material from GD2 *, there is no evidence for carnivore damage on the leporid and hyrax remains and the sample size is too small to discuss skeletal part representation. The few *H. makapanensis* and *H. africaeaustralis* elements that display evidence of digestive corrosion and gnawing indicate the consumption of some remains by medium to large carnivores. These elements could have been consumed inside or in close proximity to the cave. However, leopards feeding on small mammals, typically consume most of the carcass, with the exception of the craniodental region (Brain 1981). The abundance of *Hystrix* postcranial material counters the hypothesis of a primarily predator-accumulated porcupine assemblage.

Large mammal carcasses: accumulation scenarios

Interment and reworking of GD 2 assemblage*

We noted limited evidence for subaerial weathering on the faunal remains, which could indicate for instance that the material was sufficiently shaded by surrounding vegetation (many specimens also have fine rootlet impressions on them) and not affected by long-term exposure before being buried into the cave sediments. This is also consistent with a scenario where bones experienced only a short period of environmental exposure, for example in the case of carcasses being dragged into deeper parts of the cave by a predator, or in the case of animals falling into a natural death-trap. Further interpretation of weathering stages is limited by the lack of actualistic data regarding the rate of weathering in karstic systems in comparison to that of an open landscape.

Repeated cycles of calcification/decalcification, as well as exposure to erosion after the cave deposits were exposed to the surface likely explain the high degree of fragmentation in the assemblage. Within the highly fragmented assemblage, small elements dominate, which might reflect some degree of post-depositional sorting through gravity, remobilization of sediments (e.g. karstic subsidence) or water action. This could be an indication that the recovered specimens do not fully represent the faunal assemblage in its primary depositional context. Regarding possible water action, there is only limited evidence for hydrological transport. While we agree with Pickering (1999) that the lack of clear signs of hydrological sorting on bone cortical surfaces does not always equate with the absence of hydrologic action, the equally well-represented elements from the lag group and easily transported elements within the GD 2* fauna provides further support to the hypothesis of limited fluvial transport. An alternative hypothesis could be that the material was transported only over a short distance before final deposition and/or by a gentle flow (Fernández-Jalvo & Andrews 2003; Fernández-Jalvo *et al*. 2014).

Manganese dioxide deposits on the GD 2* assemblage are generally quite thick and coat most of the specimens. Thackeray (2016) suggests that manganese coatings could be the result of lichen deposited on bone and rock surfaces, which are absorbing manganese from the surrounding dolomitic substrates. These lichens prefer the half-dark, damp areas of caves (the 'twilight zone'), where growth is extensive. Following this hypothesis, one possibility would be that the GD 2* fossils spent some time in the 'twilight zone' of Gondolin cave, given the extensive degree of manganese coating observed on the specimens. More generally, manganese coatings form preferably on rocks and bones in environments where decalcification of cave breccia is occurring (Cukrowska *et al*. 2005). Thus, their abundance on the GD 2* material

might also result from the fact that it comes from decalcified sediments.

There is a tendency for compact and denser bones to be overrepresented in the GD 2* assemblage compared to fragile elements. While the statistical tests we performed do not support a direct correlation between bone density and survivorship of skeletal elements, we suggest that this is probably affected by the under-representation of the dense shafts of long bones. Because of the high fragmentation rate of the GD 2* assemblage, most long bone shaft fragments are likely included within the non-identifiable remains; their underrepresentation in the bovid sample is thus an analytical bias rather than the reflection of true absence. This phenomenon is well documented in some archaeological and palaeontological assemblages (see for instance Bartram & Marean 1999). The presence of delicate or fragile skeletal elements in the assemblage could indicate a relatively quick interment of the material since prolonged exposure to accumulation and post-depositional processes would have destroyed them. While these fragile skeletal remains are few in GD 2*, their presence furthers supports the argument that at least a portion of the material was deposited into the GD 2* section of the cave soon after death rather than having spent time outside where the material would have been exposed to the environment and various dispersal agents.

Carnivore contribution to the GD 2 assemblage*

The most commonly identified ungulates from the GD 2* assemblage are medium-sized bovids from the tribe Reduncini (*Redunca arundinum*, *R. fulvorufula* and *Redunca* sp.), while bovid class sizes I and II make up the majority of the unidentified bovid material. This is consistent with modern leopard kills that illustrate a clear bodyweight bias towards small to medium-bodied bovids (Hirst 1969; Grobler & Wilson 1972; Brain 1981; Bailey 1993). Hyaenas are opportunistic predators and their prey spectrum usually resembles an attritional mortality profile, while as ambush predators leopards tend to produce catastrophic mortality profiles (e.g. Kruuk 1972; Stiner 1990). The latter is in line with the mortality profiles documented for the GD 2* bovids I and II. Because felids do not typically disarticulate their prey, a felid-accumulated assemblage usually preserves some complete and articulated remains, (Smith 1977; Bailey 1993). As mentioned before, there are no articulated remains, or any complete remains (beyond carpals, tarsals, sesamoids and phalanges) in the GD 2* assemblage. This could be due to secondary sorting of the material, as discussed above. Sesamoids, carpals and tarsals are all small, compact and highly durable bones, generally better preserved in the fossil record. The %MAU values for bovid classes I and II have a similar distribution that suggests that these two bovid size classes were subjected to similar accumulation and post-depositional processes. Hyaena-accumulated assemblages are generally characterized by heavily consumed elements, including chewed-up long bone epiphyses and more intense gnawing and digestion damage. In contrast, large felids primarily deflesh their prey, usually leaving long bones intact and epiphyses ungnawed (e.g. Brain 1981; de Ruiter & Berger 2000), except for the occasional tooth pits or scores where the teeth may have scraped against the bone during feeding. The GD 2* assemblage displays no heavily consumed elements and many epiphyseal heads of long bones were found intact. Besides, there is no clear indication that hyaenids used the GD 2* cave as a denning site. The low carnivore to ungulate ratio (7.4%) of the GD 2* assemblage falls well below the 20% value that Cruz-Uribe (1991), Pickering (2002) and Kuhn *et al*. (2010) recommend to be the cut-off for determining whether an assemblage was accumulated by hyaenas or not. Secondly, only two dental hyaenid specimens were recovered and we did not find coprolites or juvenile hyaenid material during the excavation. Carnivore damage on the total assemblage is limited and we did not identify bone cylinders. Finally, the relatively good representation of long bone epiphyses speaks against intense carcass ravaging by hyaenids. Notwithstanding these observations, several studies highlight that distinguishing between leopards and hyaenas' taphonomic signature is not always straightforward (e.g. Arriaza *et al*. 2019), notably in the case of secondary scavenging by the latter. In such a scenario, hyaena damage to the carcasses may be less visible than in the case of primary accumulation by this predator. In the case of GD 2*, the lack of bone cylinders might simply result from bone attrition due to natural post-depositional fragmentation processes (e.g. calcification/decalcification cycles). Furthermore, leopards consume carcasses in a different way compared to lions and there is not a uniform felid-consumption model (e.g. Domínguez-Rodrigo *et al*. 2007). For instance, leopards do consume the proximal parts of long bones, notably the tibiae. We conclude that the most likely scenario is a primary accumulation of most small to medium bovid carcasses (sizes I and II) by a leopard-like carnivore but that further investigation of carnivore damage could shed some light on a possible secondary scavenging by other carnivores, including hyaenids and/or smaller carnivores.

The remains of larger bovids (size classes III and IV) are scarce and comprise mostly craniodental elements. Processes other than carnivore predation possibly brought this material into the cave system (e.g. slope wash, gravity). The occurrence of gnawing damage does, however, suggest some degree of carnivore scavenging either inside or outside of the karstic system. Interestingly, while the abundant primate material from several Plio-Pleistocene sites such as Swartkrans Members 1 to 3, Kromdraai B and Member 2 and Sterkfontein Member 4 (Brain 1981, 1993; de Ruiter 2001; Pickering *et al*. 2004a,b; Fourvel *et al*. 2018) is regarded as the result of leopard-accumulation, there are no primate remains in the GD 2* assemblage. When adding the faunal samples from GD 1, GD 2, GD 2* and GD A, the total faunal assemblage from Gondolin comprises 21 416 remains (Table 8), which includes a single cercopith bone (from GD A; Adams *et al*. 2018). This is interesting, considering that modern large-bodied primates occupy habitats similar to those reconstructed for the Gondolin area (Menter *et al*. 1999; Adams 2006).

Comparison of GD 2* fauna with other *Paranthropus robustus*-bearing sites in the Cradle of Humankind

Intra-site comparison

Albeit much smaller, the GD 2 * faunal assemblage is most similar to the GD 2 one (Table 8). The taxonomic composition of both assemblages is similar and the GD 2* assemblage shares comparable distribution of bovid size classes and a relatively low McIntosh evenness index with GD 2 (Table 8). In both assemblages, the bovid sample is biased towards small to medium bovids, with bovids size class II clearly dominating in both cases. The low McIntosh evenness indexes indicate that both GD 2 and GD 2* display a narrow taxonomic range, with an assemblage composed mostly of bovids (with abundant Reduncini), the distinct absence of primates and a low number of carnivores. GD 1 has a higher evenness index, related to a lower number of taxa that are more evenly distributed (Adams *et al*. 2007). GD A has the highest evenness value – in fact, the highest when compared to other Cradle sites (Table 8) – and a higher carnivore to ungulate ratio, two elements that reflect its wider variety of taxa encompassing several species of carnivores, primates, hominins and bovids. GD A is an *ex situ* dump that possibly contains mixed material from multiple localities (Adams 2018). The taxonomic and taphonomic similarities between the faunal assemblages from GD2* and GD 2 are to be expected given the proximity of both fossil deposits within the Gondolin locality. We suggest that GD 2* represents the decalcified fraction of the same fossil deposit from which the calcified sediments of GD 2 were excavated.

Inter-site comparison

The provenience of the material (e.g. decalcified *versus* calcified sediments; and *in situ* versus *ex situ* deposits), as well as the excavation and fossil preparation methods are likely to have influenced the taxonomic composition of the fossil assemblages under consideration. Similarly, there are clear differences in sample size (Table 8) between them. We therefore urge the considerations that we propose below to be regarded with caution. GD 2* is most similar in its distribution of bovid size classes to Kromdraai B, Sterkfontein (Member 5 Oldowan Infill/East Infill) and Cooper's D (Table 7). GD 2*'s McIntosh evenness index (0.68) is lower than that of all other fossil localities considered here, with the exception of GD 2, which has an even lower value. Other *P. robustus*-bearing sites in the Cradle of Humankind present higher evenness values, comprised between 0.71 (Drimolen Main Quarry) and 0.82 (Swartkrans M2). A high evenness value is associated with a wider variety of taxa encompassing several species of carnivores, primates, hominins and bovids. The low McIntosh evenness index of the GD 2* assemblage reflects its relatively low taxonomic diversity and the over-representation of Reduncini. The carnivore to ungulate ratios of the Cradle of Humankind sites range from 15.3% to 39.8%, and GD 2* falls far below this number at only 7.4%.

CONCLUSION

Taxonomic analysis indicates that the macrofaunal assemblage recovered from the decalcified sediments of the GD 2* deposits contains mostly ungulates, some small mammals and very few carnivore remains. We identified four species, not previously identified in the Gondolin assemblages. These include: two bovid species, *Alcelaphus* cf. *buselaphus* and *Redunca fulvorufula*, the springhare (*Pedetes capensis*), and the barn owl (*Tyto alba*). No hominin or non-hominin primate remains were found. The identification of *Equus* sp., *Hystrix makapanensis* and *Metridiochoerus andrewsi* specimens provides a biochronological bracket for the assemblage of 2.33–1.78 Ma. The assemblage displays a taxonomic and bodyweight bias towards

Table 8. Intra- and inter-site comparisons with percentages of size classes for the bovid assemblages (data in % bovid NISP, except for Cooper's D where the data are presented in MNI and % bovid MNI), McIntosh evenness indexes and carnivore-ungulate ratios for Gondolin and other *Paranthropus robustus*-bearing assemblages in the Cradle of Humankind.

Assemblage	NISP	Bov I	Bov II	Bov II/III	Bov III	Bov IV	Evenness	Carn/ung. ratio	Sources
GD 2*	1259	32.3	58.5	–	8.7	0.4	0.68	7.4	This study
GD 2	16477	28.3	69.2	–	2.4	0.1	0.60	4.85	Adams (2010)
GD A	2292	10.2	46.0	–	42.6	3.0	0.90	9.1	Adams (2018)
GD 1	1388	7.1	39.3	–	53.6	0	0.79	0	Adams *et al.* (2007)
Sterkfontein M5 East Infill	3731	27.0	48.7	–	18.9	5.4	0.75	16.1	Pickering (1999)
Kromdraai B	~800	18.8	49.8	–	30.5	1.0	0.77	30.0	Brain (1981)
Kromdraai M2**	2444	(small) 36.7		–	(medium) 56.6	(large) 6.7	0.80	39.8	Fourvel *et al.* (2018)
Swartkrans M1 (HR)	1162	2.9	41.4	–	52.9	2.9	0.81	24.3 (15.0)	Watson (1993b); Adams (2010)
Swartkrans M2	5570	2.5	49.4	–	43.2	4.9	0.82	19.3 (16.5)	Watson (1993b) Adams (2010)
Swartkrans M3	3236	4.3	47.1	–	45.0	3.6	0.81	23.2 (20.9)	Watson (1993b); Adams (2010)
Cooper's D	200	1.0	37.0	–	55.0	7.0	0.74	27.7	de Ruiter *et al.* (2009)
Drimolen Main Quarry	1380	9.9	41.2	34.4	11.5	3.1	0.71	27.3	Adams *et al.* (2016)

**Fourvel *et al.* (2018) use a different size class system than Brain (1974).

small-bodied bovids (size classes I and II) and this is consistent with the taphonomic analysis, which indicates the selective action of a leopard-like carnivore that either dragged bovid carcasses into the cave whole or fed on them from a tree overhanging the cave mouth. Porcupines made a small contribution to the assemblage, although it is not clear whether they brought in material from outside the cave or modified the material that was already present. No clear correlation between bone density and bone preservation could be determined, but this might be a consequence of the high degree of fragmentation within the assemblage. The size classes III and IV material might have been introduced into the assemblage through other processes, such as slope wash or gravity, and their small sample size does not allow for a detailed taphonomic assessment. The assemblage of small mammals is most likely a product of these taxa using the site as habitat, with a minor contribution by carnivores feeding on them. An intra- and inter-site comparison between the GD 2* assemblage and other *P. robustus*-bearing sites in the Cradle of Humankind revealed a close resemblance to the GD 2 assemblage in terms of bovid size class distribution, species diversity, a low carnivore to ungulate ratio and the absence of primate remains. This indicates similarities in terms of assemblage formation processes, both likely originating from the same deposits (calcified in the case of GD 2 and decalcified in the case of GD 2*).

The support of the DST-NRF Centre of Excellence in Palaeosciences (CoE-Pal), the National Research Foundation (NRF), the African Origins Platform and the Palaeontological Scientific Trust (PAST) towards this research is hereby acknowledged. Opinions expressed, and conclusions arrived at, are those of the authors and are not necessarily to be attributed to the CoE-Pal or NRF. Further thanks are extended to the following individuals and institutions for their assistance during the course of this research: Dr Shaw Badenhorst and Dr Heidi Fourie from the Ditsong National Museum of Natural History in Pretoria, for granting access to the Archaeozoology and Plio-Pleistocene collections, and Dr Bernhard Zipfel from the Evolutionary Studies Institute (University of the Witwatersrand), for facilitating access to the Quaternary Collection and microscope laboratories. Analysis of the Gondolin fossil material will not be possible without the volunteers who helped during the fieldwork and we express here special thanks to Tumelo Molefyane. Finally, we would like to thank Brigette Cohen for detailed and constructive corrections on a previous version of this manuscript, as well as a second anonymous reviewer for valuable comments.

§ORCID iDs

M. Engelbrecht: orcid.org/0000-0002-2895-2025
A. Val: orcid.org/0000-0001-5350-186X
C. Steininger: orcid.org/0000-0002-9082-0672

REFERENCES

ADAMS, J.W. 2006. *Taphonomy and Paleoecology of the Gondolin Plio-Pleistocene Cave Site, South Africa*. Ph.D. thesis, Washington University in St. Louis.

ADAMS, J.W. 2010. Taphonomy of the Gondolin GD 2 in situ deposits and its bearing on interpretations of South African Plio-Pleistocene karstic fossil assemblages. *Journal of Taphonomy* **8**, 81–116.

ADAMS, J.W. 2012a. Stable carbon isotope analysis of fauna from the Gondolin GD 2 fossil assemblage, South Africa. *Annals of the Ditsong National Museum of Natural History* **2**, 1–5.

ADAMS, J.W. 2012b. Craniodental and postcranial remains of the extinct porcupine *Hystrix makapanensis* Greenwood, 1958 (Rodentia, Hystricidae) from Gondolin, South Africa. *Annals of the Ditsong National Museum of Natural History* **2**(1), 7–17.

ADAMS, J.W. 2018. Fossil mammals from the Gondolin Dump A *ex situ* hominin deposits, South Africa. *PeerJ* **6**, e5393.

ADAMS, J.W. & CONROY, G.C. 2005. Plio-Pleistocene faunal remains from the Gondolin GD 2 in situ assemblage, North West Province, South Africa. **In**: Lieberman, D., Smith, R.J., Kelley, J. (eds), *Interpreting the Past, Essays on Human, Primate and Mammal Evolution in Honour of David Pilbeam*, pp. 243–261. Boston, Brill Academic Publishers Inc.

ADAMS, J.W., HERRIES, A.I.R., CONROY, G.C. & KUYKENDALL, K.L. 2007. Taphonomy of a South African cave, geological and hydrological influences on the GD 1 fossil assemblage at Gondolin, a Plio-Pleistocene paleocave system in the Northwest Province, South Africa. *Quaternary Science Review* **26**, 2526–2543.

ADAMS, J.W., ROVINSKY, D.S., HERRIES, A.I.R. & MENTER, C.G. 2016. Macromammalian faunas, biochronology and palaeoecology of the early Pleistocene Main Quarry hominin-bearing deposits of the Drimolen Palaeocave System, South Africa. *PeerJ* **4**, e1945.

ARMSTRONG, A. & AVERY, G. 2014. Taphonomy of verreaux's eagle (*Aquila verreauxii*) prey accumulations from the Cape Floral Region, South Africa: implications for archaeological interpretations. *Journal of Archaeological Science* **52**, 163–183.

ARRIAZA, M.C., ARAMENDI, J., MATÉ-GONZÁLEZ, M.Á., YRAVEDRA, J. & STRATFORD, D. 2019. Characterising leopard as taphonomic agent through the use of micro-photogrammetric reconstruction of tooth marks and pit to score ratio. *Historical Biology*. DOI: 10.1080/08912963.2019.1598401

BACKWELL, L.R., PARKINSON, A.H., ROBERTS, E.M., D'ERRICO, F. & HUCHET, J.B. 2012. Criteria for identifying bone modification by termites in the fossil record. *Palaeogeography, Palaeoclimatology, Palaeoecology* **337-338**, 72–87.

BAILEY, T. 1993. *The African Leopard: Ecology and Behavior of a Solitary Felid*. New York, Columbia University Press.

BARTRAM, L.E. & MAREAN, C.W. 1999. Explaining the "Klasies Pattern": Kua ethnoarchaeology, the Die Kelders Middle Stone Age archaeofauna, long bone fragmentation and carnivore ravaging. *Journal of Archaeological Science* **26**, 9–29.

BEHRENSMEYER, A.K. 1978. Taphonomic and ecologic information from bone weathering. *Paleobiology* **4**(2), 150–162.

BERGER, L.R. & CLARK, R.J. 1995. Eagle involvement in accumulation of the Taung child fauna. *Journal of Human Evolution* **29**(3), 275–299.

BERGER, L.R., KEYSER, A.W. & TOBIAS, P.V. 1993. Brief communication, Gladysvale, first early hominid site discovered in South Africa since 1948. *American Journal of Physical Anthropology* **92**, 107–111.

BERGER, L.R., DE RUITER, D.J., STEININGER, C.M. & HANCOX, J. 2003. Preliminary results of excavations at the newly investigated Coopers D deposit, Gauteng, South Africa. *South African Journal of Science* **99**, 276–278.

BERNOR, R.L., ARMOUR-CHELU, M.J., GILBERT, H., KAISER, T.M. & SCHULZE, E. 2010. 35. *Equidae*. **In**: Werdelin, L. & Saunders, W.J. (eds), *Cenozoic Mammals of Africa*, 685–721. Berkley, University of California Press.

BRAIN, C.K. 1974. Some suggested procedures in the analysis of bone accumulations from southern African Quaternary sites. *Annals of the Transvaal Museum* **29**, 1–8.

BRAIN, C.K. 1981. *The Hunters or the Hunted? Introduction to African Cave Taphonomy*. Chicago, University of Chicago Press.

BRAIN, C.K. 1993. A taphonomic overview of the Swartkrans fossil assemblages. **In**: Brain, C.K. (ed.), *Swartkrans: a Cave's Chronical of Early Man*, 257–264. Pretoria, Transvaal Museum.

COHEN, B.F. & KIBII, J.M. 2015. Experimental study of bone modification by captive caracal (*Caracal caracal*); a model for fossil assemblage analysis. *Journal of Archaeological Science* **62**, 92–104.

CRUZ-URIBE, K. 1991. Distinguishing hyaena from hominid bone accumulations. *Journal of Field Archaeology* **18**, 467–486.

CUKROWSKA, E.M., McCARTHY, T.S., POLE, S., BACKWELL, L. & STEININGER, C. 2005. The chemical removal of manganese coatings from fossil bones from the Cradle of Humankind, South Africa. *South African Journal of Science* **101**, 1–3.

DE RUITER, D.J. 2001. *A methodological analysis of the relative abundance of hominids and other macromammals from the site of Swartkrans, South Africa*. Ph.D. thesis, University of the Witwatersrand, Johannesburg.

DE RUITER, D.J. 2003. Revised faunal lists for Member 1-3 of Swartkrans, South Africa. *Annals of the Transvaal Museum* **40**, 29–41.

DE RUITER, D.J. & BERGER, L. 2000. Leopards as taphonomic agents in dolomitic caves – Implications for bone accumulations in the hominid bearing deposits of South Africa. *Journal of Archaeological Science* **27**, 665–684.

DE RUITER, D.J., PICKERING, R., STEININGER, C.M., KRAMERS, J.D., HANCOX, P.J., CHURCHILL, S.E., BERGER, L.R. & BACKWELL, L. 2009. New *Australopithecus robustus* fossils and associated U-Pb dates from Cooper's Cave (Gauteng, South Africa). *Journal of Human Evolution* **56**, 497–513.

DOMÍNGUEZ-RODRIGO, M., BARBA, R. & EGELAND, C.P. 2007.

Deconstructing Olduvai. A Taphonomic Study of the Bed I Sites. Dordrecht, Netherlands, Springer Books.
DOMÍNGUEZ-SOLERA, S.D. & DOMÍNGUEZ-RODRIGO, M. 2009. A taphonomic study of bone modification and of tooth-mark patterns on long limb bone portions by suids. *International Journal of Osteoarchaeology* **19**, 345–363.
ESTES, R. 1991. *The Behavior Guide to African Mammals*. Berkley, University of California Press.
FERNÁNDEZ-JALVO, Y. & ANDREWS, P. 2003. Experimental effects of water abrasion on bone fragments. *Journal of Taphonomy* **1**(3), 147–163.
FERNÁNDEZ-JALVO, Y., ANDREWS, P., SEVILLA, P. & REQUEJO, V. 2014. Digestion vs. abrasion features in rodent bones. *Lethaia* **47**, 323–336.
FERNÁNDEZ-JALVO, Y. & ANDREWS, P. 2016. *Atlas of Taphonomic Identifications: 1001+ Images of Fossil and Recent Mammal Bone Modification*. Springer.
FISHER, J.W. 1995. Bone modifications in zooarchaeology. *Journal of Archaeological Method and Theory* **2**(1), 7–69.
FOURVEL, J.B., THACKERAY, J.F., BRINK, J.S., O'REGAN, H. & BRAGA, J. 2018. Taphonomic interpretations of a new Plio-Pleistocene hominin-bearing assemblage at Kromdraai (Gauteng, South Africa). *Quaternary Science Reviews* **190**, 81–97.
GOMMERY, D., BADENHORST, S., POTZE, S., SÉNÉGAS, F., KGASI, L. & THACKERAY, J. F. 2012. Preliminary results concerning the discovery of new fossiliferous sites at Bolt's Farm (Cradle of Humankind, South Africa). *Annals of the Ditsong National Museum of Natural History* **2**, 33–45.
GROBLER, J. & WILSON, V. 1972. Food of the leopard *Panthera pardus* (Linn.) in the Rhodes Matopos National Park, Rhodesia, as determined by faecal analysis. *Arnoldia* **5**, 1–9.
HARRIS, J.M. & WHITE, T.D. 1979. Evolution of the Plio-Pleistocene African Suidae. *Transaction of the American Society* **69**(2), 1–128.
HERRIES, A. 2003. *Magnetostratigraphic seriation of South African hominin palaeocaves*. Unpublished Ph.D. thesis, University of Liverpool, Liverpool, UK.
HERRIES, A.I.R., CURNOE, D. & ADAMS, J.W. 2009. A multi-disciplinary seriation of early *Homo* and *Paranthropus* palaeocaves in southern Africa. *Quarternary International* **202**(1-2), 14–28.
HERRIES, A.I.R., ADAMS, J.W., KUYKENDALL, K.L. & SHAW, J. 2006. Speleology and magnetobiostratigraphic chronology of the GD 2 locality of the Gondolin hominin-bearing paleocave deposits, North West Province, South Africa. *Journal of Human Evolution* **51**(6), 617–631.
HERRIES, A.I.R. & ADAMS, J.W. 2013. Clarifying the context, dating and age range of the Gondolin hominins and *Paranthropus* in South Africa. *Journal of Human Evolution*
http://dx.doi.org/10.1016/j.jhevol.2013.06.007
HIRST, S. 1969. Predation as a regulating factor of wild ungulate populations in a Transvaal lowveld nature reserve. *Zoologia africana* **4**, 199–230.
KINGDON J. 1997. *The Kingdon Field Guide to African Mammals*. London, Academic Press.
KLEIN, R.G. & CRUZ-URIBE, K. 1984. *The Analysis of Animal Bones from Archaeological Sites*. Chicago, University of Chicago Press.
KUHN, B.F., BERGER, L.R. & SKINNER, J.D. 2010. Examining criteria for identifying and differentiating fossil faunal assemblages accumulated by hyenas and hominins using extant hyenid accumulations. *International Journal of Osteoarchaeology* **20**(1), 15–35.
KRUUK, H. 1972. *The Spotted Hyena. A Study of Predation and Social Behavior*. Chicago, University of Chicago Press.
LAM, Y.M., CHEN, X. & PEARSON, O. 1999. Intertaxonomic variability in patterns of bone density and the differential representation of bovid, cervid, and equid elements in the archaeological record. *Society for American Archaeology* **64**(2), 343–362.
LLOVERAS, L., MORENO-GARCIA, M., & NADAL, J. 2008. Taphonomic study of leporid remains accumulated by the Spanish imperial eagle (*Aquila adalberti*). *Geobios* **41**(1), 91–100.
LLOVERAS, L., MORENO-GARCÍA, M., & NADAL, J. 2012. Assessing the variability in taphonomic studies of modern leporid remains from eagle owl (*Bubo bubo*) nest assemblages: the importance of age of prey. *Journal of Archaeological Science* **39**(12), 3754–3764.
LYMAN, R.L. 1994a. *Vertebrate Taphonomy*. Cambridge Manuals in Archaeology. Cambridge, Cambridge Universit.
LYMAN, R.L. 1994b. Quantitative units and terminology in zooarchaeology. *American Antiquity* **59**(1), 36–71.
LYMAN, R.L., HOUGHTON, L.E. & CHAMBERS, A.L. 1992. The effect of structural density on marmot skeletal representation in archaeological sites. *Journal of Archaeological Science* **19**, 557–573.
MAGUIRE, J.M. 1976. *A taxonomic and ecological study of the living and fossil Hystricidae with particular reference to southern Africa*. Unpublished Ph.D. thesis, University of the Witwatersrand, 530–655.
MAGUIRE, J.M., PEMBERTON, D. & COLLET, M. 1980. The Makapansgat Limeworks Grey Breccia, hominids, hyaenas, hystricids, or hill wash? *Palaeontologia africana* **23**, 75–98.
McINTOSH, R. 1967. An index of diversity and the relation of certain aspects of diversity. *Ecology* **48**, 392–404.
MENTER, C.G., KUYKENDALL, K.L., KEYSER, A.W. & CONROY, G.C. 1999. First record of hominid teeth from the Plio-Pleistocene site of Gondolin, South Africa. *Journal of Human Evolution* **37**, 299–307.
O'REGAN, H.J., BISHOP, L.C., LAMB, A., ELTON, S. & TURNER, A. 2005. African faunal change. **In**: Head, M.J. & Gibbard, P.L. (eds), *Early-Middle Pleistocene Transitions: the Land-Ocean Evidence*, 242. London, Geological Society of London.
PICKERING, T.R. 1999. *Taphonomic interpretations of the Sterkfontein early hominid site (Gauteng, South Africa) reconsidered in light of recent evidence*. Unpublished Ph.D. thesis, University of Wisconsin, Madison.
PICKERING, T.R. 2002. Reconsideration of criteria for differentiating faunal assemblages accumulated by hyenas and hominids. *International Journal of Osteoarchaeology* **12**, 127–141.
PICKERING, T.R., CLARKE, R.J., MOGGI-CECCHI, J. 2004a. Role of carnivores in the accumulations of the Sterkfontein Member 4 hominid assemblage, a taphonomic reassessment of the complete hominid fossil sample (1936-1999). *American Journal of Physical Anthropology* **125**, 1–15.
PICKERING, T.R., DOMÍNGUEZ-RODRIGO, M., EGELAND, C. & BRAIN, C.K. 2004b. Beyond leopards, tooth marks and the contribution of multiple carnivore taxa to the accumulation of the Swartkrans Member 3 fossil assemblage. *Journal of Human Evolution* **46**, 595–604.
PICKFORD, M. 2013a. The diversity, age, biogeographic and phylogenetic relationships of Plio-Pleistocene suids from Kromdraai, South Africa. *Annals of the Ditsong National Museum of Natural History* **3**(1), 11–32.
PICKFORD, M. 2013b. Locomotion, diet, body weight, origin and geochronology of *Metridiochoerus andrewsi* from the Gondolin Karst Deposits, Gauteng, South Africa. *Annals of the Ditsong National Museum of Natural History* **3**(1), 33–47.
REYNARD, J.P., DISCAMPS, E., BADENHORST, S., VAN NIEKERK, K. & HENSHILWOOD, C.S. 2016. Subsistence strategies in the southern Cape during the Howiesons Poort: taphonomic and zooarchaeological analyses of Klipdrift Shelter, South Africa. *Quaternary International* **404**, 2–19.
RICHARDSON, P.R.K. 1980. Carnivore damage to antelope bones and its archaeological implications, *Palaeontologia africana* **23**, 109–125.
SHIPMAN, P. & ROSE, J. 1983a. Early hominid hunting, butchering, and carcass processing behaviours, approaches to the fossil record. *Journal of Anthropological Archaeology* **2**, 57–98.
SHIPMAN, P. & ROSE, J. 1983b. Evidence of butchery and hominid activities at Torralba and Ambrona, an evaluation using microscopic techniques. *Journal of Archaeological Science* **10**, 465–474.
SKINNER, J.D. & CHIMIMBA, C.T. 2005. *The Mammals of the Southern African Sub-region*. Cambridge University Press.
SMITH, R. 1977. Movement patterns and feeding behaviour of leopard in the Rhodes Matopos National Park, Rhodesia. *Arnoldia* **8**, 1–15.
STINER, M. C. 1990. The use of mortality patterns in archaeological studies of hominin predatory adaptations. *Journal of Anthropological Archaeology* **9**, 305–351.
THACKERAY, J.F. 2016. The possibility of lichen growth on bones of *Homo naledi*: were they exposed to light? *South African Journal of Science* **112**(7/8), 1–5.
VAL, A., TARU, P. & STEININGER, S. 2014. New taphonomic analysis of large-bodies primate assemblage from Cooper's D, Bloubank Valley, South Africa. *South African Archaeological Bulletin* **199**, 49–58.
VILLA, P. & MAHIEU, E. 1991. Breakage patterns of human long bones. *Journal of Human Evolution* **21**, 27–48.
VOORHIES, M.R. 1969. Taphonomy and population dynamics of an early Pliocene vertebrate fauna, Know County, Nebraska, *University of Wyoming Contributions to Geology* Special Paper **1**, 1–69.
VRBA, E.S. 1982. Progress Report: Gondolin Site, Broederstroom Permit 3/102. Transvaal Museum Document #3/6/9/1.
WATSON, V. 1993a. Glimpses from Gondolin: a faunal analysis of a fossil site near Broederstroom, Transvaal, South Africa. *Palaeontologica africana* **30**, 35–42.
WATSON, V. 1993b. Composition of the Swartkrans bone accumulations, in terms of skeletalparts and animals represented. **In**: Brain, C.K. (ed.), *Swartkrans: a Cave's Chronicle of Early Man*. 35–74. Pretoria, Transvaal Museum.
ZIPFEL, B. & BERGER, L.R. 2009. New Cenozoic fossil-bearing site abbreviations for collections of the University of the Witwatersrand. *Palaeontologica africana* **44**, 77–81.